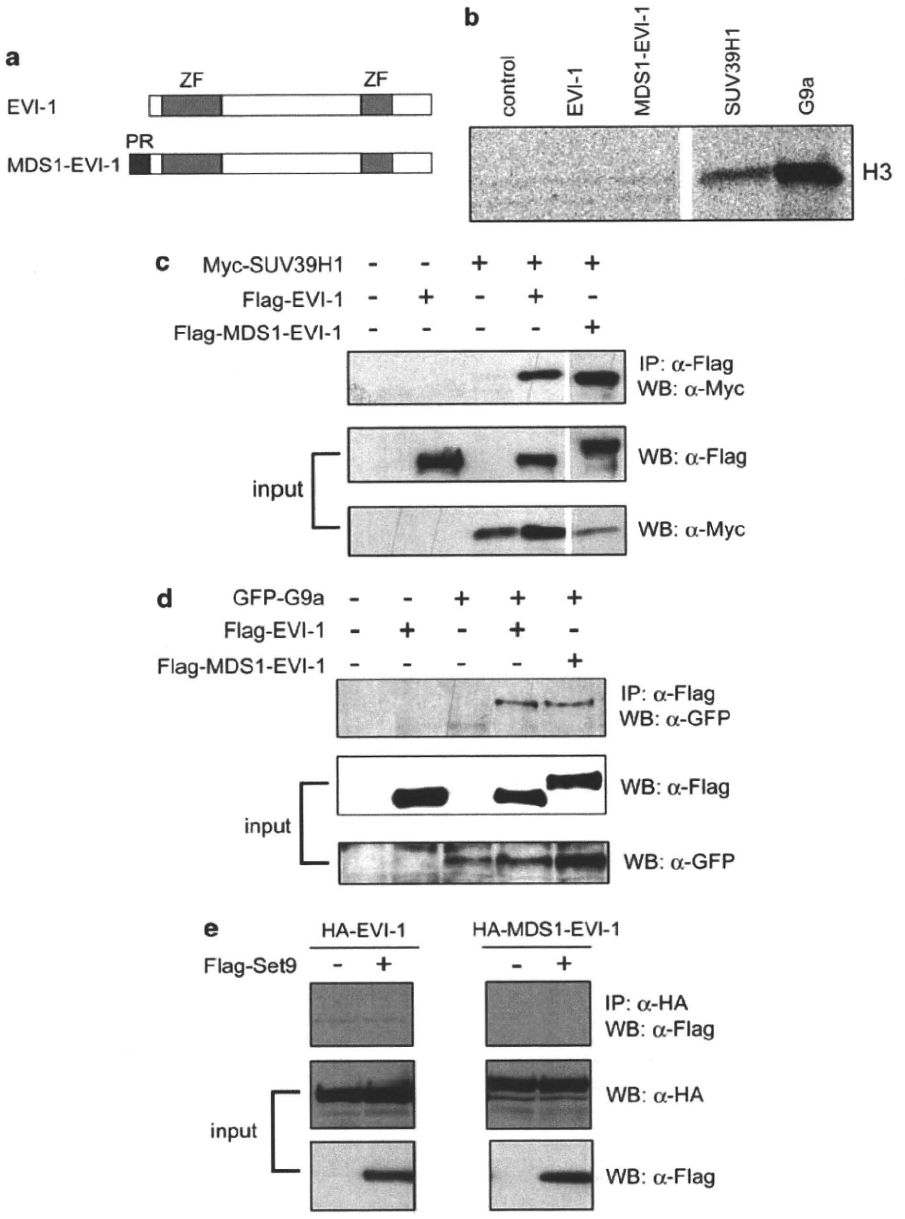

Figure 1 EVI-1 interacts with histone methyltransferases SUV39H1 and G9a, but not with Set9. (**a**) Schematic representation of EVI-1 isoforms. ZF, zinc finger domain; PR, PR domain. (**b**) Histone methyltransferase assay with FLAG-EVI-1 and Flag-MDS1-EVI-1. Lysates from cells transfected with EVI-1 or MDS1-EVI-1 were immunoprecipitated with anti-Flag antibody and analysed for specific histone H3 methylation activity by autoradiography, but neither EVI-1 nor MDS1-EVI-1 methylated histone H3. Myc-SUV39H1 and HA-G9a were purified with anti-Myc or HA antibodies and used as positive controls. (**c**) The 293T cells were transfected with Flag-EVI-1 (lanes 2 and 4), Flag-MDS1-EVI-1 (lane 5), and Myc-SUV39H1 (lanes 3–5). Whole-cell extracts were immunoprecipitated with anti-Flag antibody. Flag-EVI-1-bound Myc-SUV39H1 was detected by western blotting by means of anti-Myc (top). Expression of Flag-EVI-1 and Myc-SUV39H1 is monitored with anti-Flag (middle) and anti-Myc (bottom), respectively. (**d**) The 293T cells were transfected with Flag-EVI-1 (lanes 2 and 4), Flag-MDS1-EVI-1 (lane 5), and GFP-G9a (lanes 3–5). Whole-cell extracts were immunoprecipitated with anti-Flag antibody. Flag-EVI-1-bound GFP-G9a was detected by western blotting by means of anti-GFP (top). Expression of Flag-EVI-1 and GFP-G9a is monitored with anti-Flag (middle) and anti-GFP (bottom), respectively. (**e**) The 293T cells were transfected with HA-EVI-1 (left panel), HA-MDS1-EVI-1 (right panel) and Flag-Set9 (lane 2 of both panels). Whole-cell extracts were immunoprecipitated with anti-HA antibody. HA-EVI-1-bound Flag-Set9 was detected by western blotting by means of anti-Flag (top). Expression of HA-EVI-1 and Flag-Set9 is monitored with anti-HA (middle) and anti-Flag (bottom), respectively.

HMT assay

Flag-EVI-1, Myc-SUV39HA or HA-G9a was immunoprecipitated with anti-Flag, anti-Myc and anti-HA antibodies, respectively. The immunoprecipitates were incubated for 1 h at 37 °C in 50 μl of MAB buffer (50 mM Tris, pH 8.5, 20 mM KCl, 10 mM MgCl2, 10 mM β-mercaptoethanol, 250 mM sucrose) containing 2 μg of histone 3 (Roche, Indianapolis, IN, USA) as the substrate and *S*-adenosyl-[methyl-14C]-l-methionine as the methyl donor. Reactions were stopped by boiling the samples in sodium dodecyl sulphate loading buffer, and then the proteins were separated by

15% sodium dodecyl sulphate-polyacrylamide gel electrophoresis. Gels were dried and quantification of methyl-^{14}C was performed using a BAS-2000 imaging analyzer (Fuji Film).

Immunoprecipitation and western blotting

The 293T cells were transfected by the calcium phosphate method. The cells were cultured 48 h after transfection and were lysed in the TNE buffer.[14] For immunoprecipitation, cell lysates were incubated with the anti-Flag M2 monoclonal antibody (F3165, Sigma, St Louis, MO, USA) for 3 h at 4 °C. Then, the samples were incubated with protein-G-Sepharose (Amersham Pharmacia Biotech, Piscataway, NJ, USA) for 1 h at 4 °C. The precipitates were washed five times with the TNE buffer, subjected to sodium dodecyl sulphate-polyacrylamide gel electrophoresis, and analysed by western blotting. Western blotting was performed with anti-Flag M2-Peroxidase (A8592, Sigma), anti-Myc (2276, Cell Signaling Technology, Beverly, MA, USA), anti-HA-Peroxidase (12CA5, Roche), anti-GFP antibody (G1544, Sigma), anti-EVI-1 (C50E12, Cell Signaling Technology), anti-SUV39H1 (MG44, upstate) or anti-G9a antibody (C6H3, Cell Signaling Technology). Proteins were visualized by the enhanced chemiluminescence system (Amersham Pharmacia Biotech).

Immunofluorescence microscopy

For colocalization studies, COS7 cells were transfected with Myc-SUV39H1 or GFP-G9a together with Flag-EVI-1 using the FuGENE transfection reagent (Roche). After 48 h, cells were fixed in 3.7% formaldehyde and permealized with 0.1% Triton X-100. Samples were blocked with 1% bovine serum albumin for 40 min, incubated with mouse anti-Myc-FITC (F2047, Sigma) or rabbit anti-Flag antibody (F7425, Sigma) for 2 h, washed, and then incubated with the Alexa Fluor 555 conjugated goat anti-rabbit antibody. For evaluation of endogenous H3K9 methylation status, MEF cells were incubated with rabbit anti-dimethyl H3K9 (29698, Upstate) or rabbit anti-trimethyl H3K9 antibody (31855, Upstate), followed by labelling with Alexa Fluor 488 conjugated anti-rabbit antibody. Nuclear staining was performed using TOPRO3 (Invitrogen, Carlsbad, CA, USA). Cells were analysed by the confocal laser scanning microscopy (Leica TCS SL).

Luciferase reporter assay

For analysis of luciferase activities, 293T cells were seeded in 12-well culture plates at a density of 1×10^5 per well. At 12 h after seeding, the cells were transfected with 500 ng of p3TP-Lux, 100 ng of pME-EVI-1, and increasing amounts (100 or 200 ng) of either pcDNA3-SUV39H1, pcDNA3-SUV39H1-H324K, pcDNA3-G9a or pcDNA3-G9a-NH903/904LE using Lipofectamin 2000 (Invitrogen). The cells were harvested 48 h after transfection and assayed for the luciferase activity by means of the luciferase assay system (Promega, Madison, WI, USA) and a luminometer (Lumat, LB 9700, Berthold, Bad Wildbad, Germany). Transfection efficiency was evaluated by cotransfecting 10 ng of a reporter CMV-βgalactosidase plasmid.

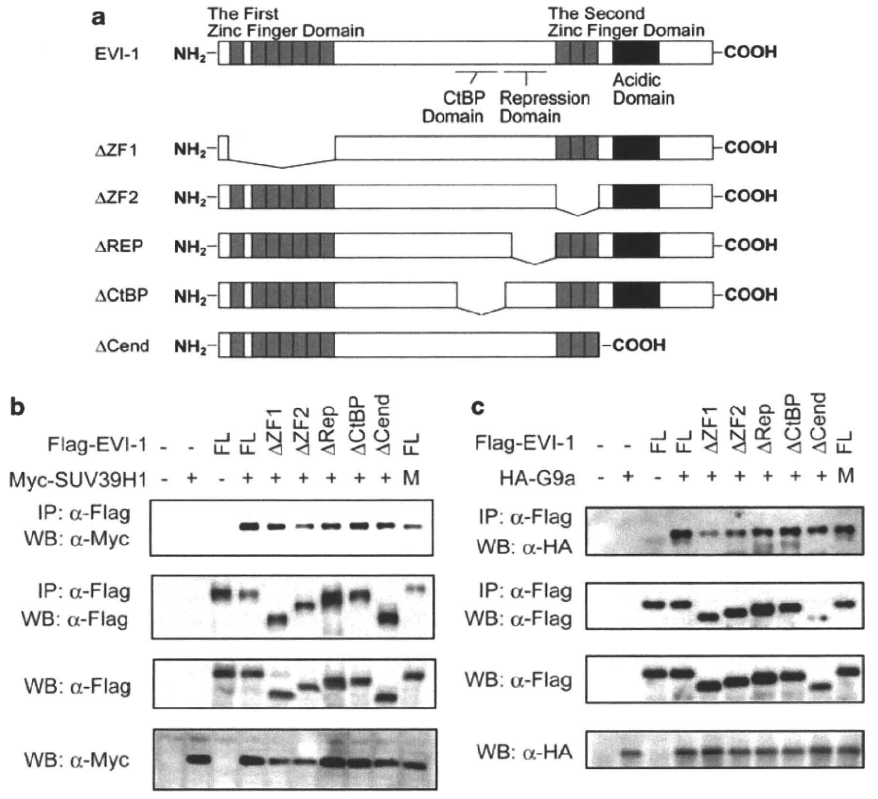

Figure 2 Domain contribution of EVI-1 for interaction with SUV39H1 and G9a. (**a**) Schematic presentation of the functional domains of EVI-1 and structures of the deletion mutants. (**b**) Association between Flag-EVI-1 or its deletion mutants and Myc-SUV39H1 or its mutant. M, a mutant carrying an inactivating point mutation within the HMT domain of SUV39H1 (SUV39H1-H324K). (**c**) Association between Flag-EVI-1 or its deletion mutants and HA-G9a or its mutant. M, a mutant carrying an inactivating point mutation within the HMT domain of G9a (G9a-NH903/904LE).

Retrovirus transduction and colony-replating assay

Plat-E packaging cells[23] were transiently transfected with 3 μg of retrovirus vectors, mixed with 9 μl of FuGENE 6 (Roche) for retrovirus production. Colony-replating assay was performed as described earlier.[24] Colony-forming cells from the third to fifth round of plating were subsequently infected with retrovirus encoding either Suv39H1-small hairpin RNA (shRNA), G9a-shRNA or control-shRNA, and the cells were replated at 1×10^5 per plate in M3434 in the presence of 1 μg/ml puromycin. Puromicin-resistant colonies were then replated at 5×10^3 per plate.

RNA interference

We designed retrovirus vectors (RNAi-Ready pSIREN-RetroQ Vector, Clontech, Palo Alto, CA, USA) encoding an shRNA directed against murine Suv39h1 or G9a. As a control, we used an shRNA vector without hairpin oligonucleotides. Reduced expression of Suv39H1 or G9a in Evi-1- or E2A/HLF-immortalized cells was confirmed by performing quantitative PCR with Universal ProbeLibrary Reference Gene Assays (Roche). Target sequences for shRNAs and primer sequences for quantitative PCR are shown in Supplementary Table 1.

Statistical analysis

Statistical significance of differences between parameters was assessed using Welch's *t*-test.

Results

EVI-1 associates with SUV39H1 and G9a in mammalian cells

As PR domain is homologous to the catalytic SET domains of HMTs, we initially assessed whether MDS1-EVI-1 (PR-containing form) is able to transfer methyl groups onto histones. We purified recombinant full-length EVI-1 and MDS1-EVI-1 from 293T cell extracts by immunopurification and analysed them by an *in vitro* HMT assay with histone H3 as a substrate. However, the immunoprecipitated EVI-1 protein (both EVI-1 and MDS1-EVI-1) had no methyltransferase activity (Figure 1b), indicating that MDS1-EVI-1 itself is not a HMT. We then investigated whether EVI-1 can associate with H3K9-specific HMTs, SUV39H1 and G9a in mammalian cells. We introduced Flag-tagged EVI-1 or MDS1-EVI-1 in the absence or presence of Myc-SUV39H1 into 293T cells. Cell lysates were subjected to immunoprecipitation with anti-Flag, followed by immunoblotting with anti-Myc. We observed that Myc-SUV39H1 was coprecipitated with both Flag-EVI-1 and Flag-MDS1-EVI-1 (Figure 1c). Using the same assay, we also found that GFP-G9a could be detected in immunoprecipitates of both Flag-EVI-1 and Flag-MDS1-EVI-1 (Figure 1d). In contrast, Flag-SET9 did not show any interaction with HA-EVI-1 (Figure 1e). Thus, both isoforms of EVI-1 are able to form a complex with two H3K9 methyltransferases, SUV39H1 and G9a.

We next mapped the region of EVI-1 that is necessary for interaction with the HMTs using EVI-1 deletion mutants that lack various functional domains (Figure 2a).[25] The first zinc

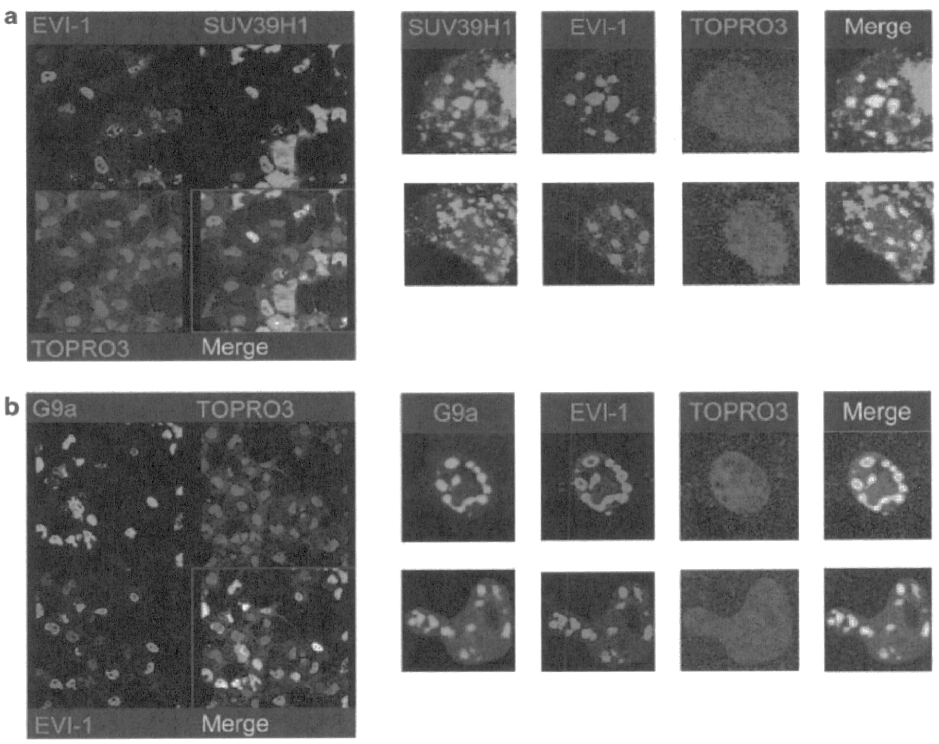

Figure 3 EVI-1 colocalizes with histone methyltransferases SUV39H1 and G9a in the nucleus. (**a**) COS7 cells were cotransfected with Myc-SUV39H1 and Flag-EVI-1 and stained with anti-Myc-FITC (green) and anti-Flag antibodies followed by secondary Alexa 555 (red) staining, together with TOPRO3 nuclei staining (blue). Merged images revealed the partial association of both proteins in speckled structures of the nucleus. (**b**) COS7 cells were cotransfected with GFP-G9a (green) and Flag-EVI-1 and stained with anti-Flag followed by secondary Alexa Fluor 555 (red) staining, together with TOPRO3 nuclei staining (blue). Merged images revealed nearly complete association of both proteins in speckled structures of the nucleus.

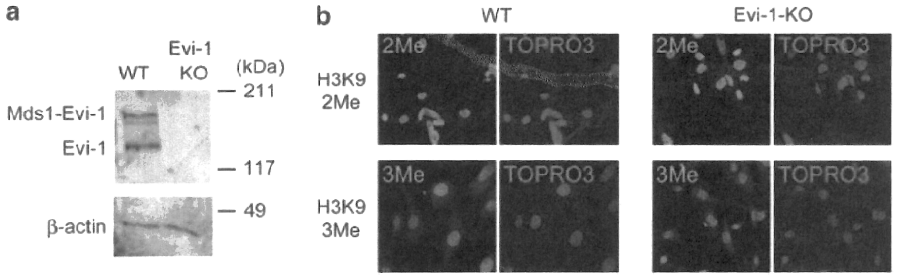

Figure 4 Evi-1 deficiency does not affect global methylation status in MEF cells. (**a**) Expression of Evi-1 and β-actin protein in wild-type and Evi-1$^{-/-}$ MEF cells. (**b**) Wild-type (left panel) and Evi-1$^{-/-}$ (right panel) MEFs were stained for H3K9-Me2 (upper panel) or H3K9-Me3 (lower panel), followed by secondary Alexa 488 (green), together with TOPRO3 nuclei staining (blue). H3K9-2Me and 3Me were broadly detected in nuclei of MEF cells, and Evi-1$^{-/-}$ cells showed no remarkable change on the overall methylation level.

finger domain (ZF1) is a DNA-binding domain and is essential for interaction with several proteins, including Smad3 and c-Jun N-terminal kinase.[5,6] The second zinc finger domain (ZF2) is another DNA-binding domain and is essential for AP-1 activation.[7] The repression domain is required for the efficient repression of TGF-β signalling.[5] The region containing CtBP-binding-motif-like sequences is responsible for the interaction with CtBP1.[16] In addition, EVI-1 contains a highly acidic domain at the C-terminus, which is required for EVI-1-mediated P-Sp haematopoiesis.[26] In contrast to the earlier reports, which showed that EVI-1 interacts with SUV39H1 through ZF1,[21,22] all of these deletion mutants associate with both SUV39H1 and G9a almost as efficiently as full-length EVI-1 (Figure 2b and c). These results indicate that the interactions between EVI-1 and HMTs are mediated through a relatively wide stretch of multiple regions, at least in 293T cells.

EVI-1 colocalizes with SUV39H1 and G9a in the nucleus

Next, we examined whether EVI-1 and the HMTs could colocalize in cells using immunofluorescence analysis with COS7 cells. Consistent with earlier reports,[27] EVI-1 shows a nuclear diffused localization pattern in the majority of cells, and sometimes shows speckled nuclear distribution (Figure 3a and b, left). When both Flag-tagged EVI-1 and Myc-tagged SUV39H1 were cotransfected into COS7 cells, EVI-1 and SUV39H1 formed speckles that partially overlap (yellow colour) in nuclei, confirming the colocalization between two proteins *in vivo* (Figure 3a, right). The possibility of cross-talk between the channels or cross-reactivity of the antibodies was ruled out (Supplementary Figure 1). The same assay also revealed nearly complete colocalization of EVI-1 and G9a in cells transfected with both constructs (Figure 3b, right). Thus, EVI-1 and the HMTs (SUV39H1 and G9a) colocalize within the nucleus in mammalian cells.

EVI-1 is not essential for the global methylation of H3K9

It has been shown that SUV39H1 is required for H3K9 trimethylation (H3K9-3Me) and G9a promotes H3K9 dimethylation (H3K9-2Me).[28] Therefore, we then examined the effect of Evi-1 deletion on the overall levels of di- and tri-methylation of H3K9 in wild-type and Evi-1$^{-/-}$ MEF cells. The absence of Evi-1 protein in Evi-1$^{-/-}$ MEF cells was confirmed by western blotting (Figure 4a). As shown in Figure 4b, H3K9-2Me and 3Me were broadly detected in nuclei of MEF cells, and Evi-1$^{-/-}$ cells showed no remarkable change on overall methylation levels. Thus, Evi-1 deficiency does not cause significant reduction of H3K9 methylation level in MEF cells.

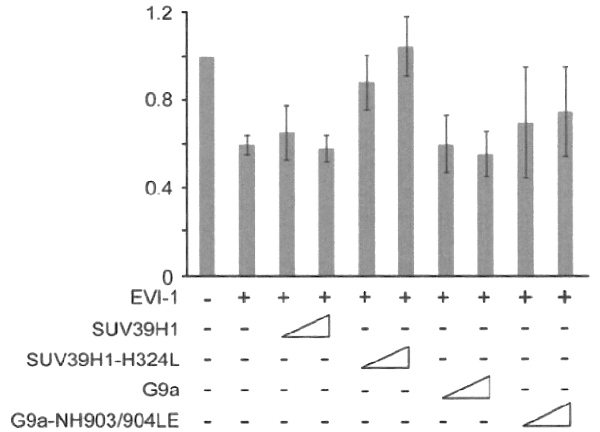

Figure 5 Transcriptional repression by EVI-1 requires catalytically active SUV39H1. The 293T cells were cotransfected with p3TP-Lux and expression vectors for EVI-1, and different concentrations of the SUV39H1, SUV39H1-H324K, G9a and G9a-NH903/904LE, as indicated. All luciferase assays were performed in triplicates in two independent experiments. Values and error bars depict the mean and the s.d., respectively.

Transcriptional repression by EVI-1 requires catalytically active SUV39H1

We next investigated whether SUV39H1 and G9a are actively involved in EVI-1-mediated transcriptional repression. We transfected 293T cells with the reporter plasmid p3TP-Lux, a synthetic TGF-β-responsive reporter that contains the promoter region of the plasminogen activator inhibitor 1 (PAI-1). As shown earlier, cotransfection of EVI-1 resulted in repression of the reporter activity. Interestingly, increasing amounts of SUV39H1-H324K, a construct carrying an inactivating point mutation within the HMT domain of SUV39H1, completely abrogated the transcriptional repression mediated by EVI-1 (Figure 5). As H324K is still able to associate with EVI-1 in immunoprecipitation studies (Figure 2b), it is thought to act as a dominant-negative mutant by competing with endogenous SUV39H1. In contrast, both G9a and G9a-NH903/904LE, a construct carrying inactivating mutations within the HMT domain of G9a, did not affect the reporter activity (Figure 5).

These results suggest that SUV39H1 is more important for EVI-1-mediated transcriptional repression in this context.

Both SUV39H1 and G9a are required for efficient propagation of Evi-1-expressing cells

We then evaluated a role for HMTs in Evi-1-induced leukemogenesis. Bone marrow cells from 5-fluorouracil-treated mice were transduced with Evi-1, and were subjected to colony-replating assay (Figure 6a). Consistent with earlier reports,[29] primary bone marrow progenitors transduced with Evi-1, but not empty vector, formed colonies in methylcellulose that can be replated through at least seven rounds of culture (data not shown). Wright-Giemsa-stained cytospin preparations of the cells constituting these Evi-1-transduced colonies showed blastic morphology with myeloid dysplasia (Figure 6b). After establishment of sustained clonogenic activity after more than three rounds of replating, the cells were transduced with Suv39h1-shRNA, G9a-shRNA or control-shRNA. We designed two independent shRNAs targeting murine Suv39H1 or G9a, and confirmed reduced expression of these HMTs by quantitative PCR in Evi-1-transduced cells and by western blotting in NIH3T3 cells (Figure 6c; Supplementary Figure 2). Although the colony-forming activity vary among different cultures (Supplementary Table 2), knockdown of Suv39h1 or G9a in Evi-1-transduced progenitors showed a clear tendency to reduce

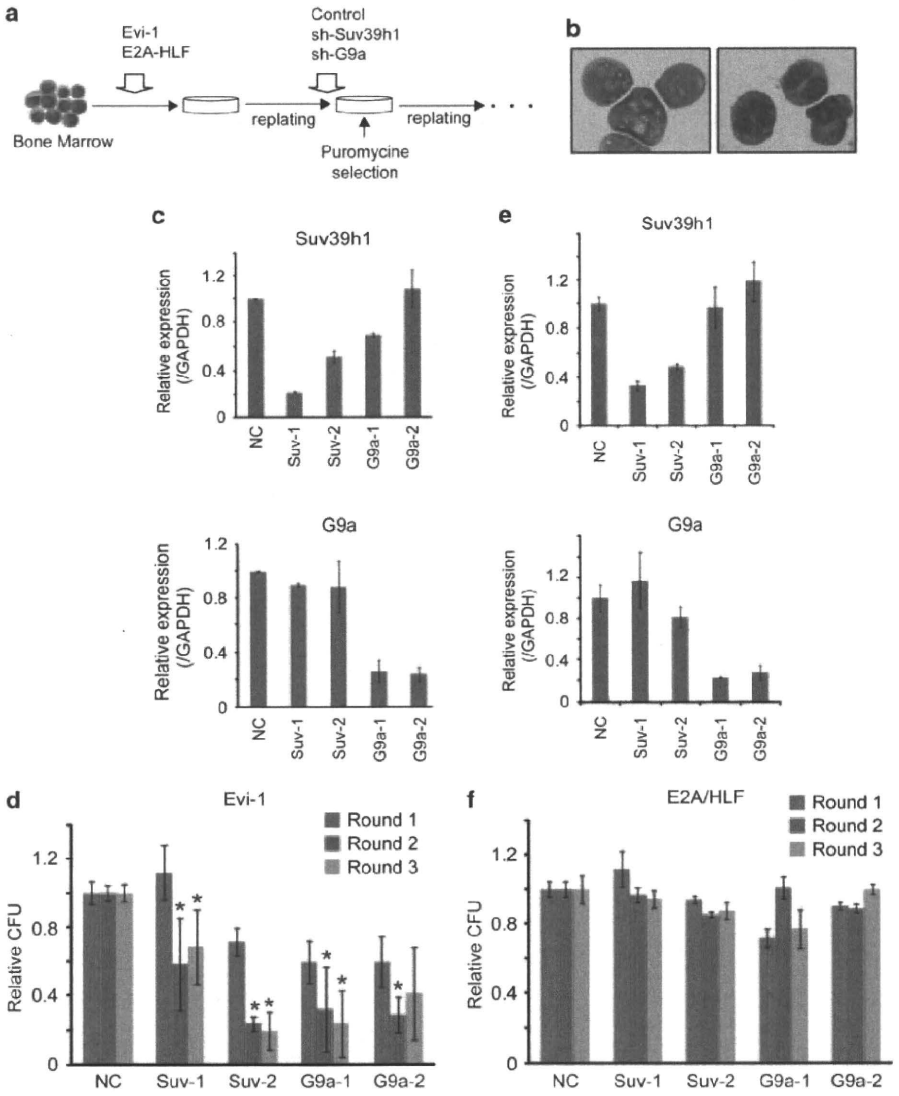

Figure 6 Effects of SUV39H1 or G9a knockdown on Evi-1-induced bone marrow immortalization. (**a**) Schematic representation of the following experiments. BM progenitors were transduced with Evi-1 or E2A/HLF oncogenes. Colony-forming cells from the third to fifth round of *in vitro* plating were subsequently transduced with Suv39h1-shRNA, G9a-shRNA or control-shRNA. Clonogenic activity was then assessed in the further round of replating in the presence of puromycin. (**b**) Giemsa-stained cells constituting colonies generated by Evi-1. Blasts (left panel) and the cells with Pseudo-Pelger-Huet anomaly (right panel) were shown. (**c**, **e**) Relative expression of Suv39h1 or G9a in Evi-1-immortalized cells (**c**) or E2A/HLF-immortalized cells (**e**) transduced with various shRNAs. Values are normalized to GAPDH. Means from two independent experiments are depicted with s.d. NC, negative control; Suv-1, 2, shRNAs for Suv39h1; G9a-1, 2, shRNAs for G9a. (**d**, **f**) Colony counts from the replating cultures of Evi-1- or E2A/HLF-immortalized cells after shRNA transduction. The bar graph shows the relative number of colonies generated by HMT-downregulated cells compared with control cells. Means from five (Evi-1) or three (E2A/HLF) independent experiments are depicted with s.d., each in duplicate. Statistical analysis was performed on Round2 and Round3 colony numbers. $*P<0.01$, relative to controls.

the colony numbers (Figure 6d; Supplementary Figure 3A; Supplementary Table 2). In addition, the HMT-knockdown cells exhibited a tendency to differentiate towards a granulocytic lineage in some experiments (Supplementary Figure 3B). We then assessed a role for the HMTs in bone marrow immortalization by E2A/HLF, a chimeric gene generated in t(17;19) that is also known to immortalize murine bone marrow cells.[30] We used E2A/HLF as a control because the contribution of Evi-1 to colony-forming ability of E2A/HLF-transduced cells is relatively small.[12] Despite the efficient downregulation of Suv39h1 and G9a (Figure 6e), the HMT-knockdown cells showed equivalent colony-forming activity to that of control E2A/HLF-transduced cells (Figure 6f; Supplementary Table 2). These results indicate that both Suv39h1 and G9a are specifically required for Evi-1-mediated bone marrow immortalization.

Discussion

Understanding mechanisms underlying EVI-1-mediated leukemogenesis is essential to develop new therapy for leukaemias with high EVI-1 expression, which are often predictive of poor clinical outcome. Very recently, it was shown that EVI-1 physically interacts with H3K9 HMTs,[21,22] suggesting that EVI-1 regulates transcription by recruiting these HMTs. Here, we extended these analyses and found that the HMTs are important for colony-replating ability of Evi-1.

The PR domain is a subclass of SET domains most closely related to the known HMTs. However, we found that MDS1-EVI-1 (PR-containing form) showed no HMT activity. It was shown earlier that PRDI-BF1 (Blimp-1), another member of PR gene family, exhibits HMT activity by recruiting G9a regardless of its PR domain.[31] Similarly, as we and others have shown, EVI-1 interacts with two HMTs, SUV39H1 and G9a. Therefore, it is likely that EVI-1 is involved in histone modification by recruiting other proteins, not through its PR domain.

Earlier reports showed that wild-type SUV39H1 enhances the repressive potential of Gal4-EVI-1 on the activity of a promoter-containing GAL4 sites, whereas the effect is not observed when the catalytically inactive mutant (SUV39H1-H324K) was used.[21,22] In contrast to these reports, we found that SUV39H1-H324K acts in a dominant-negative manner to abrogate EVI-1-mediated repression of p3TP-Lux reporter activity, whereas wild-type SUV39H1 has little effect on the repression by EVI-1. This discrepancy is probably because of the different cell types and/or promoters used for the assays. Thus, SUV39H1 is actively involved in EVI-1-mediated transcription but its effects are strictly dependent on the context. Although we did not observe significant changes in the EVI-1-mediated p3TP reporter repression by G9a or its catalytically inactive mutant (G9a-NH903/904LE), the possible requirement of G9a for EVI-1-mediated transcriptional regulation should be assessed in different experimental settings. Furthermore, because genes downregulated by EVI-1 have not been identified thus far, identification of repressive target genes of EVI-1 is an important future challenge.

Downregulation of Suv39h1 or G9a in Evi-1-transduced cells significantly inhibited their colony-forming activity. It may indicate the importance of these HMTs for generation of leukaemia-initiating cells by Evi-1. Alternatively, these HMTs may support efficient propagation of Evi-1-expressing leukaemic cells. To clarify a precise role of Evi-1/HMT complex in leukemogenesis, further *in vivo* studies are warranted. In contrast to Evi-1-induced immortalization, both Suv39h1 and G9a are dispensable for bone marrow immortalization by E2A/HLF. Although we have shown that complete loss of Evi-1 slightly reduced colony-forming ability of E2A/HLF, the effect of Evi-1 deletion in E2A/HLF-immortalized cells is relatively small than that in MLL-immortalized cells.[12] It therefore seems likely that the Evi-1/HMT interaction is not a major mediator for oncogenic activity of E2A/HLF.

Recently, several inhibitors targeting SUV39H1 and G9a have been identified.[32,33] Furthermore, we have shown that a HDAC inhibitor, trichostatin A, alleviates Evi-1-mediated repression of TGF-β signalling.[16] Therefore, combined epigenetic therapy with the HMT and the HDAC inhibitors may exert synergistic activity against EVI-1-expressing leukaemic cells, and it also needs to be evaluated in the future.

In summary, we showed that EVI-1 interacts and colocalizes with SUV39H1 and G9a. The interaction contributes, at least in part, to the transcriptional repression and bone marrow immortalization by EVI-1. Although further studies are required to address the mechanistic links between histone methylation and EVI-1-mediated leukemogenesis, our results indicate that targeting these HMTs could be of therapeutic benefit in the treatment for EVI-1-related haematological malignancies.

Conflict of interest

The authors declare no conflict of interest.

Acknowledgements

We thank T Kitamura for Plat-E packaging cells, H Nakauchi and M Onodera for pGCDNsam-eGFP retroviral vector, T Inaba, M Tachibana, Y Shinkai, K Wright and D Reinberg for cDNAs (see Materials and methods), Y Shimamura for expert technical assistance, and KYOWA KIRIN for cytokines. This work was supported in part by a Grant-in-Aid for Scientific Research from the Japan Society for the Promotion of Science, and by Health and Labour Sciences Research grants from the Ministry of Health, Labour and Welfare.

References

1 Morishita K, Parker DS, Mucenski ML, Jenkins NA, Copeland NG, Ihle JN. Retroviral activation of a novel gene encoding a zinc finger protein in IL-3-dependent myeloid leukemia cell lines. *Cell* 1988; **54**: 831–840.
2 Mucenski ML, Taylor BA, Ihle JN, Hartley JW, Morse III HC, Jenkins NA *et al.* Identification of a common ecotropic viral integration site, Evi-1, in the DNA of AKXD murine myeloid tumors. *Mol Cell Biol* 1988; **8**: 301–308.
3 Valk PJ, Verhaak RG, Beijen MA, Erpelinck CA, Barjesteh van Waalwijk van Doorn-Khosrovani S, Boer JM *et al.* Prognostically useful gene-expression profiles in acute myeloid leukemia. *N Engl J Med* 2004; **350**: 1617–1628.
4 Lugthart S, van Drunen E, van Norden Y, van Hoven A, Erpelinck CA, Valk PJ *et al.* High EVI1 levels predict adverse outcome in acute myeloid leukemia: prevalence of EVI1 overexpression and chromosome 3q26 abnormalities underestimated. *Blood* 2008; **111**: 4329–4337.
5 Kurokawa M, Mitani K, Irie K, Matsuyama T, Takahashi T, Chiba S *et al.* The oncoprotein Evi-1 represses TGF-beta signalling by inhibiting Smad3. *Nature* 1998; **394**: 92–96.
6 Kurokawa M, Mitani K, Yamagata T, Takahashi T, Izutsu K, Ogawa S *et al.* The evi-1 oncoprotein inhibits c-Jun N-terminal kinase and prevents stress-induced cell death. *EMBO J* 2000; **19**: 2958–2968.
7 Tanaka T, Nishida J, Mitani K, Ogawa S, Yazaki Y, Hirai H. Evi-1 raises AP-1 activity and stimulates c-fos promoter transactivation with dependence on the second zinc finger domain. *J Biol Chem* 1994; **269**: 24020–24026.

8 Buonamici S, Li D, Chi Y, Zhao R, Wang X, Brace L *et al.* EVI1 induces myelodysplastic syndrome in mice. *J Clin Invest* 2004; **114**: 713–719.
9 Jin G, Yamazaki Y, Takuwa M, Takahara T, Kaneko K, Kuwata T *et al.* Trib1 and Evi1 cooperate with Hoxa and Meis1 in myeloid leukemogenesis. *Blood* 2007; **109**: 3998–4005.
10 Watanabe-Okochi N, Kitaura J, Ono R, Harada H, Harada Y, Komeno Y *et al.* AML1 mutations induced MDS and MDS/AML in a mouse BMT model. *Blood* 2008; **111**: 4297–4308.
11 Yuasa H, Oike Y, Iwama A, Nishikata I, Sugiyama D, Perkins A *et al.* Oncogenic transcription factor Evi1 regulates hematopoietic stem cell proliferation through GATA-2 expression. *EMBO J* 2005; **24**: 1976–1987.
12 Goyama S, Yamamoto G, Shimabe M, Sato T, Ichikawa M, Ogawa S *et al.* Evi-1 is a critical regulator for hematopoietic stem cells and transformed leukemic cells. *Cell Stem Cell* 2008; **3**: 207–220.
13 Fears S, Mathieu C, Zeleznik-Le N, Huang S, Rowley JD, Nucifora G. Intergenic splicing of MDS1 and EVI1 occurs in normal tissues as well as in myeloid leukemia and produces a new member of the PR domain family. *Proc Natl Acad Sci USA* 1996; **93**: 1642–1647.
14 Nitta E, Izutsu K, Yamaguchi Y, Imai Y, Ogawa S, Chiba S *et al.* Oligomerization of Evi-1 regulated by the PR domain contributes to recruitment of corepressor CtBP. *Oncogene* 2005; **24**: 6165–6173.
15 Sood R, Talwar-Trikha A, Chakrabarti SR, Nucifora G. MDS1/EVI1 enhances TGF-beta1 signaling and strengthens its growth-inhibitory effect but the leukemia-associated fusion protein AML1/MDS1/EVI1, product of the t(3;21), abrogates growth-inhibition in response to TGF-beta1. *Leukemia* 1999; **13**: 348–357.
16 Izutsu K, Kurokawa M, Imai Y, Maki K, Mitani K, Hirai H. The corepressor CtBP interacts with Evi-1 to repress transforming growth factor beta signaling. *Blood* 2001; **97**: 2815–2822.
17 Palmer S, Brouillet JP, Kilbey A, Fulton R, Walker M, Crossley M *et al.* Evi-1 transforming and repressor activities are mediated by CtBP co-repressor proteins. *J Biol Chem* 2001; **276**: 25834–25840.
18 Vinatzer U, Taplick J, Seiser C, Fonatsch C, Wieser R. The leukaemia-associated transcription factors EVI-1 and MDS1/EVI1 repress transcription and interact with histone deacetylase. *Br J Haematol* 2001; **114**: 566–573.
19 Rea S, Eisenhaber F, O'Carroll D, Strahl BD, Sun ZW, Schmid M *et al.* Regulation of chromatin structure by site-specific histone H3 methyltransferases. *Nature* 2000; **406**: 593–599.
20 Tachibana M, Sugimoto K, Fukushima T, Shinkai Y. Set domain-containing protein, G9a, is a novel lysine-preferring mammalian histone methyltransferase with hyperactivity and specific selectivity to lysines 9 and 27 of histone H3. *J Biol Chem* 2001; **276**: 25309–25317.
21 Cattaneo F, Nucifora G. EVI1 recruits the histone methyltransferase SUV39H1 for transcription repression. *J Cell Biochem* 2008; **105**: 344–352.
22 Spensberger D, Delwel R. A novel interaction between the proto-oncogene Evi1 and histone methyltransferases, SUV39H1 and G9a. *FEBS Lett* 2008; **582**: 2761–2767.
23 Kitamura T, Koshino Y, Shibata F, Oki T, Nakajima H, Nosaka T *et al.* Retrovirus-mediated gene transfer and expression cloning: powerful tools in functional genomics. *Exp Hematol* 2003; **31**: 1007–1014.
24 Takeshita M, Ichikawa M, Nitta E, Goyama S, Asai T, Ogawa S *et al.* AML1-Evi-1 specifically transforms hematopoietic stem cells through fusion of the entire Evi-1 sequence to AML1. *Leukemia* 2008; **22**: 1241–1249.
25 Goyama S, Kurokawa M. Pathogenetic significance of ecotropic viral integration site-1 in hematological malignancies. *Cancer Sci* 2009; **100**: 990–995.
26 Sato T, Goyama S, Nitta E, Takeshita M, Yoshimi M, Nakagawa M *et al.* Evi-1 promotes para-aortic splanchnopleural hematopoiesis through up-regulation of GATA-2 and repression of TGF-b signaling. *Cancer Sci* 2008; **99**: 1407–1413.
27 Chakraborty S, Senyuk V, Sitailo S, Chi Y, Nucifora G. Interaction of EVI1 with cAMP-responsive element-binding protein-binding protein (CBP) and p300/CBP-associated factor (P/CAF) results in reversible acetylation of EVI1 and in co-localization in nuclear speckles. *J Biol Chem* 2001; **276**: 44936–44943.
28 Peters AH, Kubicek S, Mechtler K, O'Sullivan RJ, Derijck AA, Perez-Burgos L *et al.* Partitioning and plasticity of repressive histone methylation states in mammalian chromatin. *Mol Cell* 2003; **12**: 1577–1589.
29 Laricchia-Robbio L, Nucifora G. Significant increase of self-renewal in hematopoietic cells after forced expression of EVI1. *Blood Cells Mol Dis* 2008; **40**: 141–147.
30 Smith KS, Rhee JW, Cleary ML. Transformation of bone marrow B-cell progenitors by E2a-Hlf requires coexpression of Bcl-2. *Mol Cell Biol* 2002; **22**: 7678–7687.
31 Gyory I, Wu J, Fejer G, Seto E, Wright KL. PRDI-BF1 recruits the histone H3 methyltransferase G9a in transcriptional silencing. *Nat Immunol* 2004; **5**: 299–308.
32 Greiner D, Bonaldi T, Eskeland R, Roemer E, Imhof A. Identification of a specific inhibitor of the histone methyltransferase SU(VAR)3-9. *Nat Chem Biol* 2005; **1**: 143–145.
33 Kubicek S, O'Sullivan RJ, August EM, Hickey ER, Zhang Q, Teodoro ML *et al.* Reversal of H3K9me2 by a small-molecule inhibitor for the G9a histone methyltransferase. *Mol Cell* 2007; **25**: 473–481.

Supplementary Information accompanies the paper on the Leukemia website (http://www.nature.com/leu)

Hes1 immortalizes committed progenitors and plays a role in blast crisis transition in chronic myelogenous leukemia

Fumio Nakahara,[1-4] Mamiko Sakata-Yanagimoto,[1,2,5] Yukiko Komeno,[3,4] Naoko Kato,[3,4] Tomoyuki Uchida,[3,4] Kyoko Haraguchi,[1,6] Keiki Kumano,[1,2] Yuka Harada,[7] Hironori Harada,[8] Jiro Kitaura,[3,4] Seishi Ogawa,[9] Mineo Kurokawa,[1,2] Toshio Kitamura,[3,4] and Shigeru Chiba[1,5]

[1]Department of Cell Therapy and Transplantation Medicine and [2]Department of Hematology Oncology, University of Tokyo, Tokyo; [3]Division of Cellular Therapy, Advanced Clinical Research Center, University of Tokyo, Tokyo; [4]Division of Stem Cell Signaling, Center for Stem Cell Therapy, Institute of Medical Science, University of Tokyo, Tokyo; [5]Department of Clinical and Experimental Hematology, Graduate School of Comprehensive Human Sciences, University of Tsukuba, Ibaraki; [6]Division of Transfusion and Cell Therapy, Tokyo Metropolitan Cancer and Infectious Disease Center Komagome Hospital, Tokyo; [7]International Radiation Information Center, Hiroshima University, Hiroshima; [8]Department of Hematology and Oncology, Research Institute for Radiation Biology and Medicine, Hiroshima University, Hiroshima; and [9]Cancer Genomics Project, Graduate School of Medicine, University of Tokyo, Tokyo, Japan

Hairy enhancer of split 1 (Hes1) is a basic helix-loop-helix transcriptional repressor that affects differentiation and often helps maintain cells in an immature state in various tissues. Here we show that retroviral expression of Hes1 immortalizes common myeloid progenitors (CMPs) and granulocyte-macrophage progenitors (GMPs) in the presence of interleukin-3, conferring permanent replating capability on these cells. Whereas these cells did not develop myeloproliferative neoplasms when intravenously administered to irradiated mice, the combination of Hes1 and BCR-ABL in CMPs and GMPs caused acute leukemia resembling blast crisis of chronic myelogenous leukemia (CML), resulting in rapid death of the recipient mice. On the other hand, BCR-ABL alone caused CML-like disease when expressed in c-Kit-positive, Sca-1-positive, and lineage-negative hematopoietic stem cells (KSLs), but not committed progenitors CMPs or GMPs, as previously reported. Leukemic cells derived from Hes1 and BCR-ABL-expressing CMPs and GMPs were more immature than those derived from BCR-ABL-expressing KSLs. Intriguingly, Hes1 was highly expressed in 8 of 20 patients with CML in blast crisis, but not in the chronic phase, and dominant negative Hes1 retarded the growth of some CML cell lines expressing Hes1. These results suggest that Hes1 is a key molecule in blast crisis transition in CML. (*Blood*. 2010;115(14):2872-2881)

Introduction

The balance between activator and repressor basic helix-loop-helix transcription factors is crucial for the proper timing of cellular differentiation and normal morphogenesis of various tissues.[1] During embryogenesis, the basic helix-loop-helix protein hairy enhancer of split 1 (Hes1), functioning downstream of the Notch receptor,[2,3] blocks differentiation of neural stem cells by antagonizing Mash1[4] and affects the cell-fate decision of pancreatobiliary epithelial progenitors.[5] In the adult hematopoietic system, Hes1 blocks granulocyte colony-stimulating factor-induced granulocytic differentiation of the 32D cell line,[6] preserving the long-term reconstituting ability of hematopoietic stem cells (HSCs) in vitro as well as in vivo.[7] Hes1 also plays a significant role in the development of perinatal T cells,[8,9] and knocking out Hes1 leads to lack of thymus.[9]

Recently, activating mutations of the *Notch1* and *Notch2* genes have been identified in more than 50% of human T-cell acute lymphoblastic leukemias[10] and in a subset of non-Hodgkin lymphomas,[11] respectively, implicating Notch signal deregulation based on a genetic abnormality in human cancers. The effect of Notch signal aberration, however, has been largely confined to lymphoid lineages in the hematopoietic compartment. Indeed, enhanced Notch signaling provides the bone-marrow-to-thymus transition stage of early progenitors, with strong selective pressure toward thymic T-cell precursors at the expense of B-cell and myeloid precursors.[12-14] We recently found that up-regulation of Hes1 represents only a part of Notch signaling during the decision between mast cell and granulocyte lineage differentiation. Notch signaling does promote mast-cell development at the expense of granulocyte differentiation through up-regulation of both Hes1 and GATA-3 in common myeloid progenitors (CMPs) and granulocyte-macrophage progenitors (GMPs). However, up-regulation of Hes1 alone causes expansion of cells with myeloid progenitor phenotypes, rather than mast cell development, mediated through down-regulation of a transcription factor, C-enhancer binding protein α (C/EBP-α).[15]

A growing volume of evidence shows that down-regulation of C/EBP-α represents major events in human acute myelogenous leukemia (AML), through either genetic or epigenetic abnormalities. Therefore, it is postulated that Hes1 up-regulation may be involved in a subset of myeloid leukemias.

Chronic myelogenous leukemia (CML) is a myeloproliferative neoplasm that originates in an abnormal pluripotent bone marrow stem cell and is consistently associated with the *BCR-ABL* fusion gene. The disease is biphasic or triphasic; an initial indolent chronic phase is followed by one or both of the aggressive stages, the accelerated phase and blast crisis, resulting in expansion of immature leukemic cells. The mainstay of chronic phase to blast

Submitted May 19, 2009; accepted September 27, 2009. Prepublished online as *Blood* First Edition paper, October 27, 2009; DOI 10.1182/blood-2009-05-222836.

The online version of this article contains a data supplement.

The publication costs of this article were defrayed in part by page charge payment. Therefore, and solely to indicate this fact, this article is hereby marked "advertisement" in accordance with 18 USC section 1734.

crisis transition is the differentiation block by additional genetic events in progenitor stages of CML cells[16] that could otherwise differentiate during the chronic phase. Thus, the transformation of BCR-ABL-induced myeloproliferative neoplasm to full-blown blast crisis has been drawing tremendous attention from investigators.

Here we show that retroviral expression of Hes1 immortalizes CMPs and GMPs in vitro. Hes1 introduction together with BCR-ABL into CMPs and GMPs, the postulated origin of blast crisis transition in CML, induced CML blast crisis-like disease when intravenously administered to sublethally irradiated mice. Considering as well the study of Hes1 expression in CML patients, we propose that Hes1 is a unique experimental tool for studying the mechanisms of chronic phase to blast crisis transformation in CML.

Methods

Mice

C57BL/6 (Ly5.1) donor mice were purchased from Sankyo Labo Service Corporation. C57BL/6 (Ly5.2) recipient mice were purchased from SLC. Mice were kept at the Animal Center for Biomedical Research, University of Tokyo, according to institutional guidelines.

Bone marrow progenitor sort

Bone marrow cells were isolated from the femurs and tibias of C57BL/6 (Ly5.1) donor mice (8-10 weeks of age) and were incubated with biotinylated antibodies for lineage markers, including anti-CD3, anti-CD4, anti-CD8, anti-B220, anti-Ter119, and anti–Gr-1 antibodies (BD Biosciences PharMingen) followed by incubation with streptavidin Micro Beads (Miltenyi Biotec). The lineage marker-negative (Lin^-) fraction was separated with an autoMACS separator or LS Columns (Miltenyi Biotec) and incubated with anti-CD34–fluorescein isothiocyanate, anti-CD16/32 (FcγRIII/II receptor)–phycoerythrin (PE), anti–c-Kit–allophycocyanin, streptavidin peridinin chlorophyll protein (BD Biosciences PharMingen), and anti–Sca-1–PE/Cy7 (eBioscience). $Lin^-c\text{-}Kit^+Sca\text{-}1^+$, $Lin^-c\text{-}Kit^+Sca\text{-}1^-Fc\gamma R^{lo}CD34^+$, and $Lin^-c\text{-}Kit^+Sca\text{-}1^-Fc\gamma R^{hi}CD34^+$ cells (KSLs, CMPs, and GMPs, respectively)[17] were sorted with a FACSAria cell sorter (BD Biosciences).

Transfection and retrovirus production for murine cells

Rat Hes1 cDNA, a gift from R. Kageyama (Kyoto University, Kyoto, Japan), was subcloned into a retrovirus vector, GCDNsam/internal ribosome entry site (IRES)–nerve growth factor receptor (NGFR), a gift from H. Nakauchi (University of Tokyo) and M. Onodera (National Center for Child Health and Development, Tokyo, Japan). BCR-ABL (p210) cDNA[18] was subcloned into a retrovirus vector, GCDNsam/IRES-GFP.[19] Mouse C/EBP-α cDNA, a gift from K. Akashi (Kyushu University, Fukuoka, Japan) and S. Mizuno (Dana-Farber Cancer Institute, Boston, MA), was subcloned into a retrovirus vector, pMYs-IRES-GFP.[19] Plat-E[20] packaging cells maintained in Dulbecco modified Eagle medium supplemented with 10% fetal calf serum were transfected with retroviral constructs using FuGENE 6 transfection reagent (Roche Diagnostics) according to the manufacturer's instructions. The medium was changed a day after transfection, and retroviruses were harvested 48 hours after transfection, as previously described.[19,20]

Transfection and retrovirus production for human cell lines

We generated a dominant-negative Hes1 (dnHes1) lacking a C-terminal WRPW (Trp-Arg-Pro-Trp) domain as described.[21] The fragment of dnHes1 was subcloned into pMYs-IRES-GFP.[19] Retrovirus packaging was done as described. Briefly, retroviruses were generated by transient transfection of Plat-A[20] packaging cells with FuGENE 6 (Roche Diagnostics).

Infection to progenitors

The retrovirus medium was placed in 24-well nontissue culture dishes for 4 hours at 37°C, precoated with 40 μg/mL of RetroNectin (Takara Bio) overnight at 4°C. After washing the wells with phosphate-buffered saline, sorted KSLs, CMPs, or GMPs were plated for infection for 48 to 60 hours with the coated retroviruses harboring GCDNsam/IRES-GFP-BCR-ABL (p210) or GCDNsam/IRES-NGFR-Hes1 or an empty vector as a control. Infection was done in StemSpan SFEM medium (StemCell Technologies) containing 100 ng/mL mouse stem cell factor (SCF), 100 ng/mL mouse thrombopoietin (TPO), and 100 ng/mL human FLT3 ligand (FL) for KSLs, or in Iscove modified Dulbecco medium (Sigma-Aldrich) containing 20% fetal calf serum, 50 ng/mL mouse SCF, 20 ng/mL mouse TPO, and 20 ng/mL mouse interleukin-3 (IL-3), 20 ng/mL human IL-6 (R&D Systems) for CMPs or GMPs.

Colony-forming assay

Retrovirus-infected cells were sorted at 48 to 60 hours from the initiation of infection with a FACSAria cell sorter (BD Biosciences) and used for colony-forming assay using Methocult 3231 (StemCell Technologies), supplemented with 50 ng/mL mouse SCF, 20 ng/mL mouse TPO, and 20 ng/mL mouse IL-3, 20 ng/mL human IL-6. A total of 1000 cells were cultured in each 2.5-cm dish in duplicate. The colony-forming cells were harvested and replated every 7 to 9 days and scored for colony formation. We defined a colony as "a group of cells, grown from a single parent cell, which is composed of more than 40 live cells."

Mouse bone marrow transplantation

Bone marrow cells prepared from C57BL/6-Ly5.1 mice were infected with retrovirus containing Hes1 or BCR-ABL, and 0.1 to 2.6×10^5 of Hes1/NGFR-sorted or BCR-ABL/GFP-sorted cells were injected through tail veins into C57BL/6-Ly5.2-recipient mice (8-12 weeks of age) after sublethal (5.25 Gy) or lethal (9.5 Gy) total body γ-irradiation (^{135}Cs). For the lethally irradiated mice, 2×10^5 of C57BL/6-Ly5.2 mice-derived bone marrow cells were simultaneously injected for radioprotection. Probabilities of overall survival of the mice that received transplantations were estimated using the Kaplan-Meier method. Statistical differences were determined by the Wilcoxon test. All animal studies were approved by the Animal Care Committee of the Institute of Medical Science, University of Tokyo.

Analysis of mice receiving transplantation

After transplantation, mice were monitored for signs of disease, such as cachexia, hyperpnea, or loss of gloss in fur. Autopsies were performed on moribund recipient mice. Peripheral blood count was analyzed by KX-21 Auto Analyzer (Sysmex). Morphology of the peripheral blood was evaluated by staining of air-dried smears with Hemacolor (Merck). Tissues including bone marrow, spleen, and liver were fixed in 10% buffered formalin, embedded in paraffin, sectioned, and stained with hematoxylin and eosin. Cytospin preparations of bone marrow and spleen cells were also stained with Hemacolor. Percentage of blasts, myelocytes, neutrophils, monocytes, lymphocytes, and erythroblasts was estimated by examination of at least 200 cells. To assess whether the leukemic cells were transplantable to secondary recipients, 0.1 to 5×10^6 total bone marrow cells were injected into the tail veins of sublethally irradiated mice. Two recipient mice were used for each serial transplantation.

Flow cytometric analysis

Red blood cells were lysed using Red Blood Cell Lysing Buffer (Sigma-Aldrich) in peripheral blood or single-cell suspensions of bone marrow and spleen. After washing with phosphate-buffered saline, Fc receptor was blocked by incubating cells with 2.4G2 antibody (eBioscience) for 15 minutes at 4°C and then staining them with the following PE-conjugated monoclonal antibodies for 20 minutes at 4°C: Ly-5.1, Gr-1, CD11b, B220, CD19, CD3, CD4, CD8, c-Kit, Sca-1, CD34, and Ter119. Flow-cytometric analysis of the stained cells was performed with FACSCalibur

(BD Biosciences) equipped with CellQuest software (BD Biosciences) and FlowJo software (TreeStar).

Patients

CML patients were diagnosed at Hiroshima University Hospital and its affiliated hospitals. Diagnosis was based on morphologic, immunophenotypic, and, in some cases, real-time reverse transcription-polymerase chain reaction (RT-PCR) studies according to the French-American-British classification or World Health Organization classification. Patient samples were prepared after the research plan was approved by the Institutional Review Board at Hiroshima University, and written informed consent was obtained in accordance with the Declaration of Helsinki. Investigations were carried out in accordance with ethical standards authorized by the ethics committee of Hiroshima University and the ethics committee of the University of Tokyo (approval no. 20-10-0620)

Real-time RT-PCR

Total RNA was extracted from human bone marrow or peripheral blood cells using a TRIzol Kit (Invitrogen) according to the manufacturer's instructions, and converted to cDNA with a High Capacity cDNA Reverse Transcription Kit (Applied Biosystems). Total RNA of mouse progenitors was extracted with RNeasy (QIAGEN) according to the manufacturer's instructions, and converted to cDNA with a High Capacity cDNA Reverse Transcription Kit (Applied Biosystems). Real-time RT-PCR was performed using a LightCycler Workflow System (Roche Diagnostics). cDNA was amplified using a SYBR Premix EX Taq (Takara). Reaction was subjected to 1 cycle of 95°C for 30 seconds, 45 cycles of PCR at 95°C for 5 seconds, 58°C for 10 seconds, and 72°C for 10 seconds. All samples were independently analyzed at least 3 times. The following primer pairs were used: 5′-CCAGTTTGCTTTCCTCATTCC-3′ (forward) and 5′-TCTTCTCTCCCAGTATTCAAGTTCC-3′ (reverse) for human Hes1[22]; 5′-GAGCTGAACGGGAAGCTCACTGG-3′ (forward) and 5′-CAACTGTGAGGAGGGGAGATTCAG-3′ (reverse) for human GAPDH[22]; 5′-GAACAGCAACGAGTACCGGGTA-3′ (forward) and 5′-CCCATGGCCTTGACCAAGGAG-3′ (reverse) for mouse C/EBP-α[23]; 5′-CACAGGACTAGAACACCTGC-3′ (forward) and 5′-GCTGGTGAAAAGGACCTCT-3′ (reverse) for mouse hypoxanthine phosphoribosyltransferase (HPRT).[23] Relative gene expression levels were calculated using standard curves generated by serial dilutions of cDNA. Product quality was checked by melting curve analysis via LightCycler software (Roche Diagnostics). Expression levels were normalized by a control, the expression level of GAPDH mRNA for human samples, and HPRT mRNA for mouse samples.

Western blot analysis

To detect the expression of Hes1 or BCR-ABL (p210) proteins, equal numbers of cells from spleen or cell line were lysed, and Western blotting was performed as described with minor modifications.[24] Polyclonal rabbit anti-Hes1 antibody (H-140; Santa Cruz Biotechnology) and polyclonal rabbit anti–c-ABL antibody (K-12; Santa Cruz Biotechnology) were used for Hes1 or BCR-ABL detection, respectively.

Results

Retroviral transduction of Hes1 immortalizes CMPs and GMPs

NGFR-sorted Hes1-transduced KSLs, CMPs, and GMPs similarly generated compact and relatively large colonies, whereas empty vector-transduced KSLs generated a similar number of less large colonies. Empty vector-transduced CMPs and GMPs did not generate colonies (Figure 1A). Cytospin preparations of Hes1-transduced progenitors, stained with Hemacolor (Merck), showed blast-like morphologies, whereas those of empty vector-transduced KSLs contained bands, macrophages, and blasts (Figure 1B). Most of the empty vector-transduced CMPs and GMPs died and few cells remained (Figure 1B). In serial colony-forming assays, both CMPs and GMPs transduced with Hes1 formed colonies after at least 4 rounds of replating, with the plating efficiency more than 15% at the fourth round (Figure 1C). Replating could be reproducibly maintained for more than half a year, implying immortalizing activity of Hes1 (Figure 1D). The Hes1-transduced KSLs, CMPs, and GMPs were dependent on the presence of IL-3, requiring concentrations more than 1 ng/mL (Figure 1E; supplemental Figure 1A-B, available on the *Blood* website; see the Supplemental Materials link at the top of the online article). There was no significant difference between these cells in the dependency on IL-3. The majority of Hes1-transduced cells expressed c-Kit and CD34 at high levels, Sca-1 and CD11b at intermediate levels (Figure 1F, supplemental Figure 2A-B), irrespective of whether they were derived from KSLs, CMPs, or GMPs (supplemental Figure 2E).

The Lin^- cells were further analyzed by adopting 5-color flow cytometry that is used to identify bone marrow KSLs, CMPs, and GMPs. The expression levels of c-Kit, Sca-1, and CD34 were distributed over wide ranges. Approximately 2.5% to 6.4% of all nucleated cells showed a phenotype similar to KSLs, and another 4.8% to 11.6% showed a phenotype similar to GMPs. There were few cells that resembled CMPs (Figure 1G). We sorted the KSL-like cells, CMP-like cells, and GMP-like cells from each Hes1-transduced cell (Hes1-KSLs, Hes1-CMPs, and Hes1-GMPs) and cultured them for a week in methylcellulose. The same analysis by 5-color flow cytometry showed accumulation of GMP-like cells (~ 45.3%-83.5% of all nucleated cells) and moderate accumulation of KSL-like cells (~ 4.3%-23.4% of all nucleated cells) in the cultured cells (supplemental Figure 3A-C).

BCR-ABL replaces IL-3 in Hes1-immortalized cell lines

Because the Hes1-immortalized cell lines were IL-3 dependent for their growth in vitro, we examined whether additional signaling could replace IL-3. IL-3 signaling takes place mainly via Stat-, Ras-MAPK-, and PI3K-Akt-dependent pathways. It is also known that CML-specific BCR-ABL (p210) can replace IL-3 signaling in several experimental designs. Thus, we retrovirally expressed BCR-ABL together with Hes1. The combination of Hes1 and BCR-ABL enabled KSLs, CMPs, and GMPs to form colonies after repeated replating, not only in the presence of cytokines (Figure 2A left panel) but also in the condition free from cytokines (Figure 2A right panel). In contrast, KSLs, but not CMPs or GMPs, formed colonies by BCR-ABL transduction alone only when supplemented with cytokines (Figure 2A left panel), and they did not form any colonies without cytokines (Figure 2A right panel) or after replating with/without cytokines (Figure 2A both panels). In the liquid culture, it was shown that KSLs, CMPs, and GMPs transduced with both Hes1 and BCR-ABL were immortalized without cytokine supplementation (Figure 2B). The colonies made from Hes1- and BCR-ABL-transduced cells showed similar morphology with those from Hes1-transduced cells in the presence of a cytokine cocktail (Figure 2C). Importantly, the morphology of colony-forming cells derived from BCR-ABL-transduced KSLs was much more mature compared with those derived from Hes1- and BCR-ABL-transduced KSLs, CMPs, and GMPs, even in the same cytokine cocktail (Figure 2D). The majority of $Hes1^+$BCR-ABL^+ KSLs as well as $Hes1^+$BCR-ABL^+ CMPs and GMPs expressed CD34 at high levels, whereas they expressed c-Kit, Sca-1, and CD11b at intermediate levels (Figure 2E; supplemental Figure 2C-D), irrespective of whether they were derived from

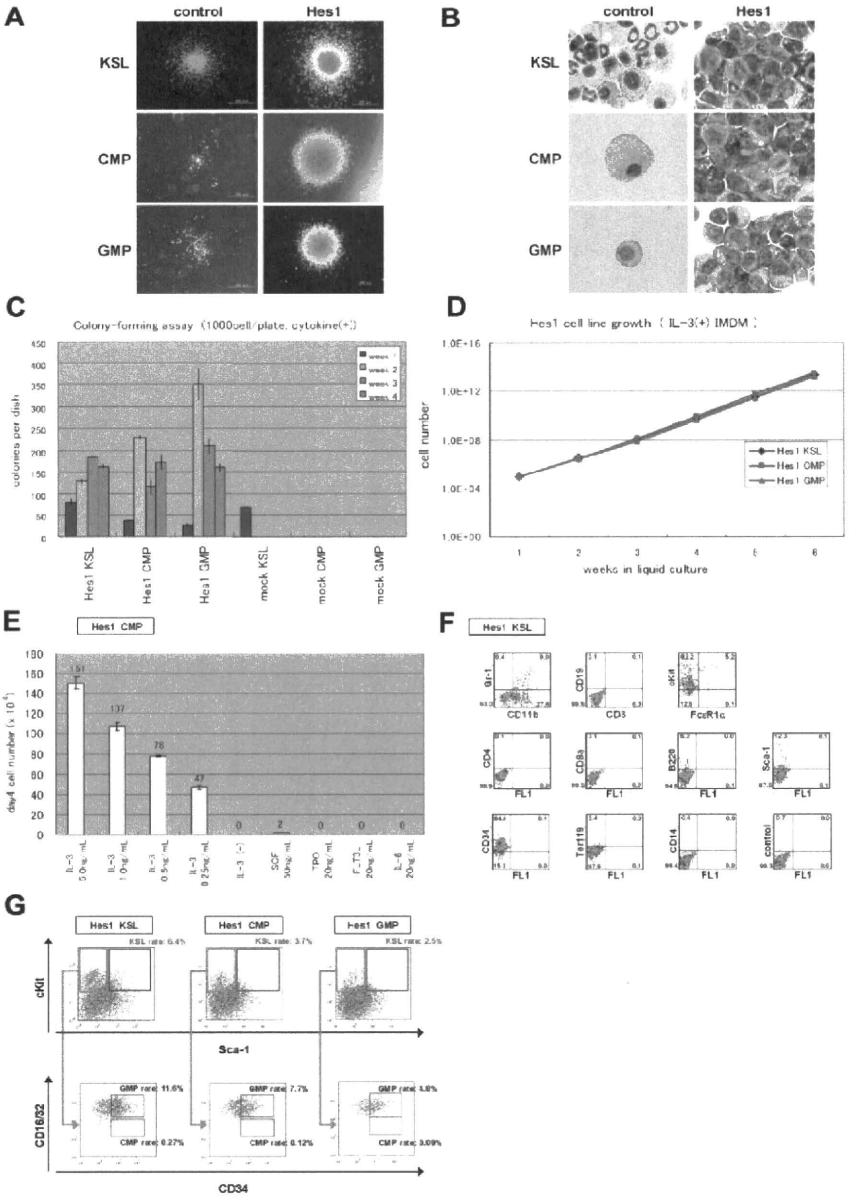

Figure 1. Hes1-transduced KSLs, CMPs, or GMPs were immortalized in the presence of IL-3. (A) Typical colonies derived from Hes1- and empty vector-transduced KSLs, CMPs, and GMPs in the presence of SCF, TPO, IL-3, and IL-6. Images were obtained with an IX70 microscope and a DP70 camera (Olympus); an objective lens, UPlanFl (Olympus); original magnification ×40 (bottom 2 in the right panels) and original magnification ×100 (remaining 4 panels). (B) Giemsa staining of Hes1- and control vector-transduced KSLs, CMPs, and GMPs. Images were obtained with a BX51 microscope and a DP12 camera (Olympus); an objective lens, UPlanFl (Olympus); original magnification ×1000. (C) Colony-forming assay from KSLs, CMPs, and GMPs transduced with Hes1 or empty vector. Hes1-transduced cells were replatable more than 4 times in vitro. Bars represent the number of colonies obtained per 10^3 cells after each round of plating in methylcellulose supplemented with SCF, TPO, IL-3, and IL-6. A representative result from 3 independent and reproducible experiments is shown. Error bars represent the SD from duplicate cultures. (D) Sustained growth of Hes1-transduced cells in liquid culture supplemented with 1 ng/mL IL-3. The number of cells was determined every 7 days by trypan blue staining, and 10^5 cells per well were seeded into a 6-well plate. Liquid culture was reproducibly continued for more than 6 months. (E) Cytokine requirement of Hes1-transduced CMPs. The cells were cultured in Iscove modified Dulbecco medium supplemented with indicated cytokines in duplicate. The numbers of cells were counted after 4 days of culture. A representative result from 2 independent and reproducible experiments is shown. Error bars represent the SD from duplicate cultures. Hes1-transduced KSLs and GMPs showed similar results (supplemental Figure 1A-B). (F) Flow-cytometric analysis of Hes1-transduced KSLs cultured in methylcellulose supplemented with SCF, TPO, IL-3, and IL-6. The dot plots represent Gr-1, CD19, c-Kit, CD4, CD8a, B220, Sca-1, CD34, Ter119, and CD14 labeled with a corresponding PE-conjugated monoclonal antibody versus CD11b, CD3, and FcεR1α labeled with a corresponding fluorescein isothiocyanate-conjugated monoclonal antibody or FL1 with no monoclonal antibody. Hes1-transduced CMPs and GMPs showed similar expression patterns (supplemental Figure 2A-B). (G) Flow-cytometric analysis of Lin$^-$-gated Hes1-transduced cells. Five-color analyses are used to identify KSL-like (top panels) and CMP-like and GMP-like cells (bottom panels) in the Hes1-transduced KSLs, CMPs, and GMPs. The number shows the percentage of cells in all nucleated cells. The analyzed cells were NGFR sorted at 48 to 60 hours from the initiation of Hes1- or control vector-transduction and cultured for the following lengths of time before the analysis: (A) 1 week, (B) 1 week, (C) 0 days, (D) 4 weeks, (E) 2 weeks, (F) 1 week, and (E) 2 weeks.

KSLs, CMPs, or GMPs (supplemental Figure 2F). Hes1$^+$BCR-ABL$^+$ KSLs, CMPs, and GMPs showed lower expressions of c-Kit and CD34 than KSLs, CMPs, and GMPs transduced with Hes1 alone (supplemental Figure 2E-F) when cultured in the presence of the same cytokine cocktail (SCF, TPO, IL-3, and IL-6). Expression of Hes1 or BCR-ABL in the Hes1 ± BCR-ABL transduced CMP or GMP cell lines was confirmed by Western blot analysis (supplemental Figure 4A).

Hes1$^+$BCR-ABL$^+$ CMPs and GMPs rapidly induce AML/CML blast crisis-like disease in recipient mice

To examine the effect of Hes1 on leukemogenesis, Hes1-transduced KSLs, CMPs, and GMPs were injected through tail veins into C57BL/6-Ly5.2 recipient mice (8-12 weeks of age) after a sublethal (5.25 Gy) or a lethal (9.5 Gy) dose of total-body γ-irradiation (^{135}Cs). For the lethally irradiated mice, 2×10^5 bone marrow cells from C57BL/6-Ly5.2 mice were simultaneously injected for radioprotection. All the mice that received transplantations of Hes1-transduced KSLs, CMPs, and GMPs were kept healthy, and no recipients developed myeloproliferative neoplasms (MPNs) or leukemias for up to 250 days after the transplantation (Figure 3A). Regarding the nonleukemogenic nature of the stem/progenitor cells transduced with Hes1 alone, we[7] and others[25] previously reported similar results, although the cell populations and/or experimental designs were not identical.

In agreement with the previous reports,[26] recipient mice injected with BCR-ABL-transduced KSLs developed fatal MPN within 30 days after the transplantation, whereas those injected with BCR-ABL-transduced CMPs and GMPs were kept healthy for more than 130 days. We did not find any signs of MPN or leukemias when mice were killed between 130 and 200 days after the transplantation (Figure 3B).

Because we found that the combination of Hes1 and BCR-ABL transduction conferred cytokine-independent immortalization on CMPs and GMPs, we injected Hes1$^+$BCR-ABL$^+$ KSLs, CMPs, and GMPs through tail veins into C57BL/6-Ly5.2 recipient mice

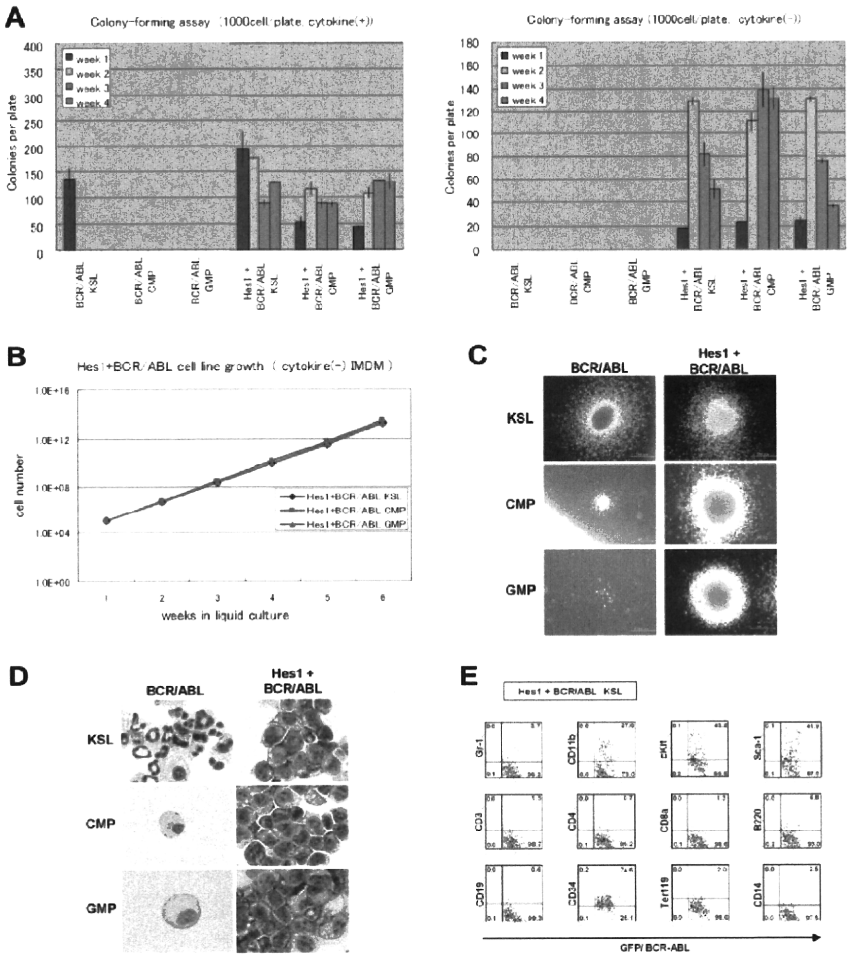

Figure 2. Hes1- and BCR-ABL-transduced KSLs, CMPs, or GMPs were immortalized independently of IL-3. (A) Colony-forming assay of KSLs, CMPs, and GMPs transduced with BCR-ABL alone or Hes1 and BCR-ABL, cultured in methylcellulose with or without cytokine cocktail containing SCF, TPO, IL-3, and IL-6. Hes1$^+$BCR-ABL$^+$ cells could be serially replated more than 4 times both with or without cytokines. In contrast, whereas KSLs, but not CMPs or GMPs, transduced with BCR-ABL alone, formed colonies in the presence of cytokines, neither KSLs, nor CMPs, nor GMPs formed colonies without cytokine supplementation. Bars represent the number of colonies obtained per 10^3 cells after each round of plating in methylcellulose. A representative result from 3 independent and reproducible experiments is shown. Error bars represent the SD from duplicate cultures. (B) Sustained growth of Hes1$^+$BCR-ABL$^+$ cells in liquid culture without cytokine supplementation. The numbers of cells were determined every 7 days by trypan blue staining, and 10^5 cells per well were seeded into a 6-well plate. Liquid culture was reproducibly continued for more than 6 months. (C) Typical colonies derived from KSLs, CMPs, and GMPs transduced with BCR-ABL alone (left panels) or BCR-ABL and Hes1 (right panels) in the presence of SCF, TPO, IL-3, and IL-6. Images were obtained with an IX70 microscope and a DP70 camera (Olympus); an objective lens, UPlanFI (Olympus); original magnification ×100. (D) Giemsa staining of Hes1$^+$BCR-ABL$^+$ KSLs, CMPs, and GMPs. Images were obtained with a BX51 microscope and a DP12 camera (Olympus); an objective lens, UPlanFI (Olympus); original magnification ×1000. (E) Flow-cytometric analysis of Hes1$^+$BCR-ABL$^+$ KSLs cultured in methylcellulose supplemented with SCF, TPO, IL-3, and IL-6. The dot plots represent Gr-1, CD11b, c-Kit, Sca-1, CD3, CD4, CD8a, B220, CD19, CD34, Ter119, and CD14 labeled with a corresponding PE-conjugated monoclonal antibody versus expression of GFP/BCR-ABL. Hes1$^+$BCR-ABL$^+$ CMPs and GMPs showed a similar expression pattern (supplemental Figure 2C-D). The analyzed cells were GFP and NGFR sorted at 48 to 60 hours from the initiation of BCR-ABL- or Hes1$^+$BCR-ABL transduction and cultured for the following lengths of time before the analysis: (A) 0 days, (B) 4 weeks, (C) 1 week, (D) 1 week, and (E) 1 week.

after sublethal irradiation. The numbers of cells injected varied among experiments, ranging from 17×10^2 to 15×10^4, because of the difference in sorting efficiencies. All the mice receiving transplantations rapidly developed fatal AML/CML in blast crisis-like disease with no significant difference in latency, ranging between 18 and 39 days after the transplantation ($P < .867$) (Figure 4A). The tissue distribution of the disease was virtually the same among mice receiving KSLs, CMPs, and GMPs; they invariably demonstrated marked hepatosplenomegaly and lung hemorrhage resulting from infiltration of leukemic cells (Figure 4B). Expression of Hes1 and BCR-ABL in the spleen cells of recipient mice was confirmed by Western blot analysis (supplemental Figure 4B).

The morphology of bone marrow demonstrated increased myeloid blasts (Figure 4C), and the histology of spleen, liver, and lungs demonstrated extensive infiltration of leukemic cells (Figure 4D). The percentages of the blasts ranged between 28% and 55% of all nucleated bone marrow cells (mean, 36.5%) of the mice receiving Hes1- and BCR-ABL-transduced KSLs, CMPs, and GMPs. In contrast, the percentages of bone marrow blasts in the recipient mice receiving BCR-ABL-transduced KSLs were only 6% to 7% (Figure 5A). White blood cell counts in the peripheral blood of recipients with Hes1$^+$BCR-ABL$^+$ KSLs, CMPs, and GMPs were $2.4 \times 10^4/\mu L$ to $67.9 \times 10^4/\mu L$ (mean, $17.8 \times 10^4/\mu L$), whereas those with BCR-ABL-transduced KSLs showed moderate leukocytosis ranging between $2.9 \times 10^4/\mu L$ and $3.8 \times 10^4/\mu L$ (Figure 5B). The surface marker profiles of the bone marrow cells from the recipients with Hes1$^+$BCR-ABL$^+$ cells expressed CD11b and Gr-1 at high levels, whereas they expressed c-Kit, Sca-1, and CD34 at intermediate levels (Figure 5C; supplemental Figure 5A-B), irrespective of whether they were derived from KSLs, CMPs, or GMPs (supplemental Figure 5C).

The long-term self-renewal properties of the leukemic cells derived from Hes1- and BCR-ABL-transduced CMPs or GMPs were tested by transplantation into secondary recipients; 0.1 to 5×10^6 total bone marrow cells were injected into the tail veins of sublethally irradiated mice. All recipient mice transplanted with more than 10^5 Hes1$^+$ cells from bone marrow developed fatal AML/CML in blast crisis-like disease with latencies of between 18 and 75 days (supplemental Figure 4C). The disease was almost identical with the primary disease (data not shown).

Hes1 expression is elevated in a substantial subset of human CML blast crisis samples

The results presented from the mouse model experiments suggest a potential link between deregulated expression of Hes1 and human CML in blast crisis. We measured the Hes1 mRNA by real-time RT-PCR in 11 peripheral blood, 1 cerebrospinal fluid, and 8 bone marrow samples from CML in blast crisis patients; 19 bone marrow samples from CML in chronic phase patients; and 10 bone marrow samples from normal subjects. In 8 of 20 CML in blast crisis samples, we found that Hes1 mRNA levels were elevated by more than 4 times the average of normal bone marrow samples (Figure

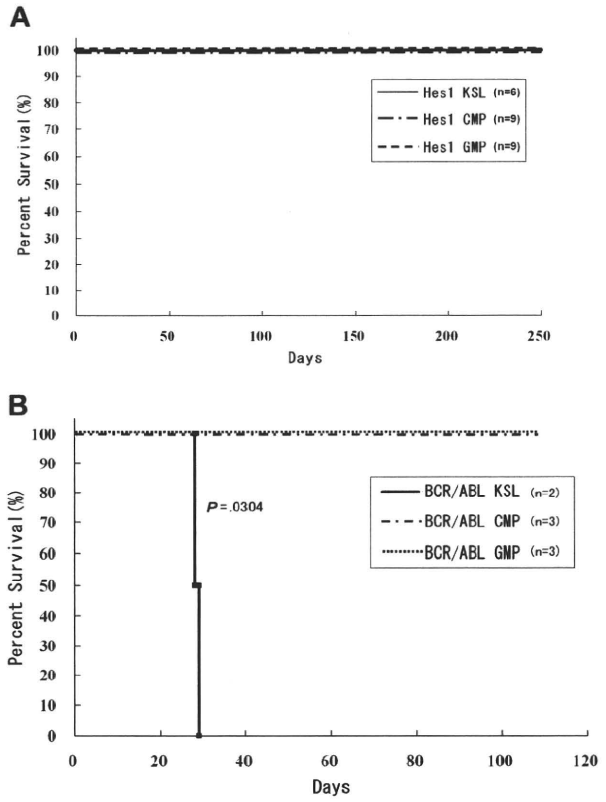

Figure 3. Mice transplanted with Hes1-transduced KSLs, CMPs, and GMPs were kept healthy. (A) Survival curves for mice injected with Hes1-transduced progenitors. No mice showed any signs of MPN for more than 250 days from transplantation. Data were analyzed by the Kaplan-Meier method. The numbers of transplanted mice are shown. Three independent experiments were performed. (B) Survival curves for mice injected with BCR-ABL-transduced progenitors. Mice transplanted with BCR-ABL-transduced KSLs developed fatal MPN within 30 days after transplantation, whereas mice transplanted with BCR-ABL-transduced CMPs or GMPs showed no evidence of disease when killed between 130 and 200 days after transplantation. Data were analyzed using the log-rank test. The 2 independent experiments were performed, and the total numbers of transplanted mice are shown.

6A). Interestingly, all but one of their phenotypes were myeloid, and 5 of 12 samples in which Hes1 mRNA levels were not elevated were derived from patients with B-cell lineage lymphoid crisis. On the other hand, the average of Hes1 mRNA levels in CML in chronic phase samples seemed to be lower than that of the normal bone marrow samples, with no sample exceeding twice the average. Clinical data of 20 patients with CML in blast crisis are shown in Table 1. The correlation coefficient between the blast percentage and the Hes1 mRNA level was −0.395, indicating that the elevated Hes1 expression level was independent of the increase in the blast percentage.

To investigate the role of Hes1 in CML blast crisis, we measured the Hes1 mRNA by real-time RT-PCR in 5 human cell lines (K-562,[27] JK-1,[28] KCL-22,[29] TS9:22,[30] and JURL-MK1[31]), which were derived from CML in blast crisis. We found that, in 3 of 5 CML blast crisis cell lines, Hes1 mRNA levels were elevated compared with the normal bone marrow sample (Figure 6B). We transduced a dominant-negative Hes1 (dnHes1) lacking a C-terminal WRPW domain via retrovirus vector into the 3 cell lines (K-562, TS9:22, and JURL-MK1) in which Hes1 mRNA levels were elevated. Indeed, in 2 of these 3 cell lines, proliferation was significantly suppressed by transduction of dnHes1 (Figure 6C). The repression of C/EBP-α by Hes1 was also observed in Hes1-transduced KSLs, CMPs, and GMPs compared with control vector-transduced KSLs, CMPs, and GMPs (Figure 6D). When C/EBP-α retrovirus vector was transduced to Hes1-transduced KSLs, CMPs, and GMPs, all of these cells differentiated to segmented neutrophils, suggesting that the expression of C/EBP-α reversed the function of Hes1 (supplemental Figure 6).

Discussion

In the present study, we demonstrated that retroviral transduction of Hes1 readily immortalizes myeloid progenitors at various stages.

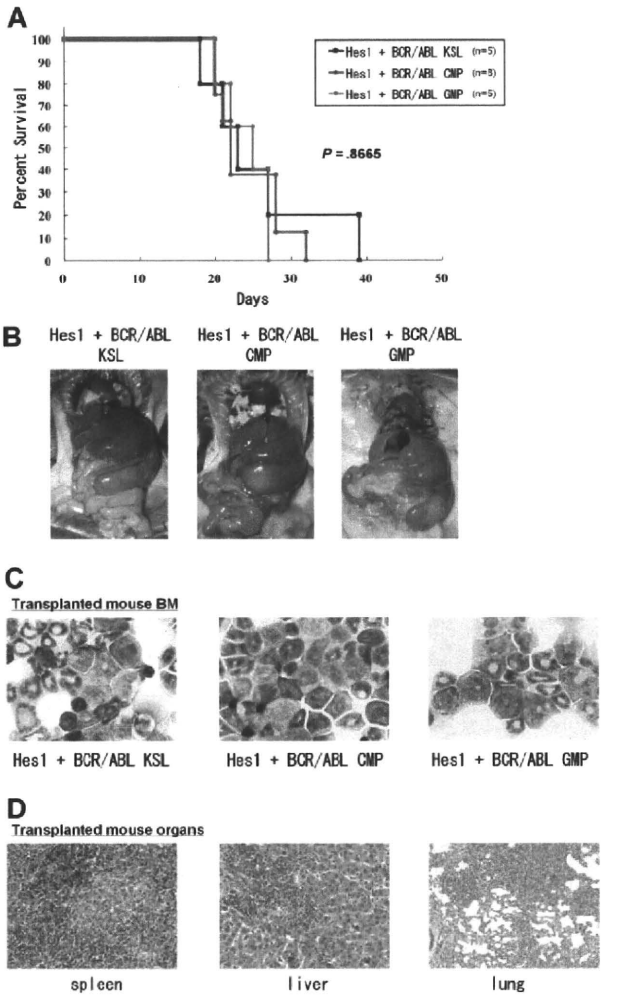

Figure 4. CMPs and GMPs transduced with the combination of Hes1 and BCR-ABL rapidly induced AML/blast crisis of CML. (A) Survival curves of mice. KSLs (n = 5), CMPs (n = 8), and GMPs (n = 5) transduced with the combination of Hes1 and BCR-ABL developed fatal AML/CML in blast crisis-like disease within 18 to 39 days, 20 to 32 days, and 20 to 27 days, respectively. Numbers of injected cells ranged 17×10^2 to 2.6×10^4 for KSLs, 5.5×10^4 to 15×10^4 for CMPs, and 4.0×10^4 to 13.8×10^4 for GMPs. There was no significant difference in latency of penetrance ($P < .867$). Statistical differences were determined using the log-rank test. Three independent experiments were performed, and the total numbers of transplanted mice are shown. (B) Tissue distribution of the leukemic cells. Mice transplanted with KSLs, CMPs, and GMPs transduced with the combination of Hes1 and BCR-ABL invariably demonstrated marked hepatosplenomegaly and lung hemorrhage, both resulting from infiltration of leukemic cells. (C) The morphology of bone marrow cells from representative recipient mice. Increased myeloid blasts were seen with no significant difference among KSLs, CMPs, and GMPs. (D) Histology of spleen, liver, and lungs from representative mice receiving Hes1$^+$BCR-ABL$^+$ GMPs. Vast infiltration of leukemic cells is seen. There were no differences in the histology among mice receiving Hes1$^+$BCR-ABL$^+$ KSLs, CMPs, and GMPs.

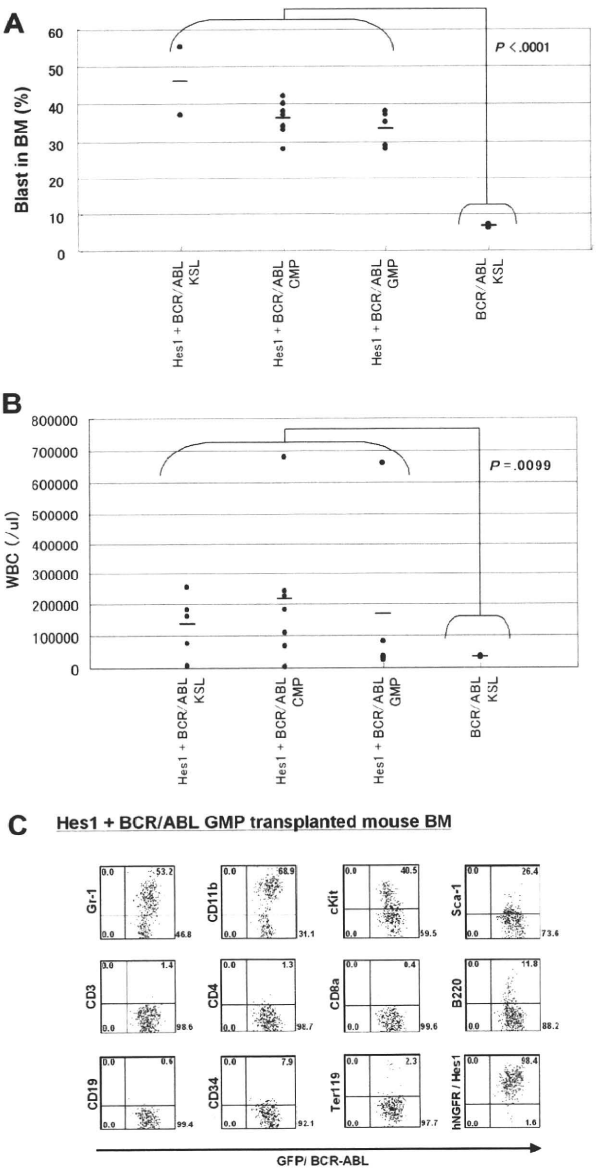

Figure 5. Comparisons of blast percentages in the bone marrow and peripheral blood leukocyte counts between mice receiving KSLs transduced with BCR-ABL alone and those receiving KSLs, CMPs, and GMPs transduced with the combination of Hes1 and BCR-ABL. (A) Blast ratios in the bone marrow. The mean blast ratios in all nucleated bone marrow cells were 6.5% ± 0.7% and 36.5% ± 6.9% in mice receiving KSLs transduced with BCR-ABL alone and in those receiving KSLs, CMPs, and GMPs transduced with the combination of Hes1 and BCR-ABL, respectively. The difference was statistically significant by the 2-sample *t* test with Welch correction ($P < .001$). (B) Peripheral white blood cell counts (WBCs). WBCs were 3.4 ± 0.6 × $10^4/\mu L$ and 17.8 ± 20.3 × $10^4/\mu L$ in mice receiving KSLs transduced with BCR-ABL alone and in those receiving KSLs, CMPs, and GMPs transduced with the combination of Hes1 and BCR-ABL, respectively. The difference was statistically significant by the 2-sample *t* test with Welch correction ($P < .001$). (C) Flow-cytometric analysis of bone marrow cells from mice receiving GMPs transduced with the combination of Hes1 and BCR-ABL. The dot plots represent Gr-1, CD11b, c-Kit, Sca-1, CD3, CD4, CD8a, B220, CD19, CD34, Ter119, and NGFR labeled with the corresponding PE-conjugated monoclonal antibody versus expression of GFP/BCR-ABL. NGFR is a marker of Hes1, and GFP is a marker of BCR-ABL transduction. The bone marrow cells derived from mice receiving KSLs or CMPs transduced with the combination of Hes1 and BCR-ABL showed essentially the same pattern (supplemental Figure 5A-B).

Moreover, when BCR-ABL is transduced together, Hes1 tranforms differentiated myeloid progenitors, such as CMPs and GMPs, in addition to hematopoietic stem cell-rich population, such as KSLs, to AML/CML in blast crisis-like cells, rapidly killing recipient mice. This result is in sharp contrast to the fact that a hematopoietic stem cell-containing population is required for BCR-ABL to cause MPN-like disease.

Hes1 is known as an effector molecule functioning downstream of Notch signaling. The activating mutations of the extracellular heterodimerization domain and/or the C-terminal PEST domain of Notch1 have been identified in approximately 50% of human T-cell acute lymphoblastic leukemias.[10,32] We have recently identified gain-of-function mutations of *Notch2* in conjunction with increased copy numbers of the mutation-carrying *Notch2* allele in a subset of B-cell lymphomas.[11] A possible association between deregulated Notch signaling is also reported in Hodgkin lymphoma, anaplastic large cell lymphoma, small-cell lung cancer, and prostate adenocarcinoma, etc.[33] Regarding myeloid malignancies, however, only one paper reports the identification of the activating mutation of Notch1 in 1 of 12 human AML samples.[34] Given that Notch signaling is among the strongest inducers of T-cell lineage commitment[12,13] and that increased Notch signaling could block myeloid lineage commitment,[15] deregulated Notch signaling might antagonize, rather than promote, the development of myeloid malignancies. However, Hes1 does not necessarily represent Notch signaling. Indeed, other extracellular signaling, such as Sonic Hedgehog,[35] could affect Hes1 expression, and cross-talk between Hes family proteins and molecules in various cell signaling pathways, such as Stat3,[36] has been demonstrated.

We previously reported that Hes1 preserved highly purified hematopoietic stem cells in vitro and contributed to the expansion of transduced hematopoietic stem cells in the recipients' bone marrow,[7] but the effect of Hes1 transduction on myeloid progenitors was not evaluated in detail. We have now found the myeloid progenitor-immortalizing activity of Hes1. In addition, accumulation of KSL- and GMP-like population in Hes1-transduced cells implicates a role for Hes1 in leukemic stem cells. On the other hand, we have also found that the in vitro growth of the Hes1-immortalized cells is dependent on cytokine signaling and that Hes1 alone is insufficient to be fully leukemogenic when overexpressed. The mainstay of the Hes1 effects on myeloid progenitors appears to be blockade of differentiation, although other functions, such as reversion from the quiescent state to the actively cycling state,[21] may also be involved. In the present study, we confirmed that Hes1 expression represses C/EBP-α, a transcription factor having important roles in myeloid differentiation, in mouse KSLs and committed progenitors as we reported.[15] Moreover, transduction of C/EBP-α reversed the differentiation block caused by Hes1 expression, which partially explains the mechanism of blocked myeloid differentiation by Hes1. C/EBP-α is frequently mutated in AML with the normal karyotype.[37-39] In other human AML without C/EBP-α mutations, reduced C/EBP-α expression, possibly through deregulated epigenetic control, is not uncommon and is associated with poor prognosis.[40,41] Furthermore, mice injected with mutated C/EBP-α-transduced bone marrow cells develop myelodysplastic syndrome and AML.[42] Therefore, reduction of C/EBP-α function is highly relevant to the development and/or progression of myeloid malignancies. Hes1, therefore, might be involved in human myeloid malignancies through suppression of C/EBP-α.

Up-regulation of Hes1 is shown in a subset of human rhabdomyosarcomas[21] and medulloblastomas.[43,44] In the present study, we have detected elevated expression of Hes1 in 8 of the 20 samples from CML in blast crisis patients, but not those from CML

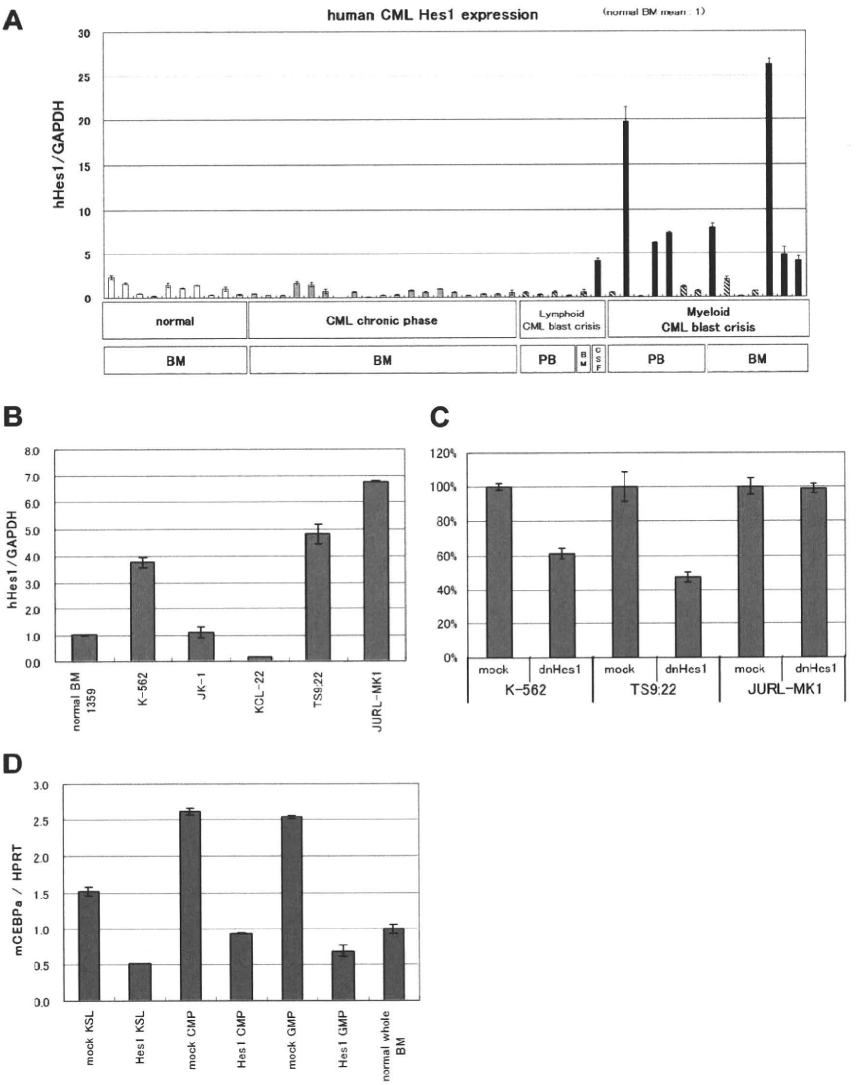

Figure 6. Hes1 expression was elevated in approximately 40% of patients with CML in blast crisis. (A) Real-time RT-PCR for Hes1 in bone marrow or peripheral blood cells from healthy subjects, patients with CML in chronic phase, or patients with CML in blast crisis. Expression levels were normalized by GAPDH mRNA. RNA from normal bone marrow cells served as a control (mean of 10 RNA levels of normal bone marrow was defined as 1). Hes1 mRNA levels exceeded 4 (solid bar) in 8 of 20 samples from CML in blast crisis patients. The correlation coefficient determined by the Wilcoxon signed-rank test between blast ratio and Hes1-expression level was −0.395. PB indicates peripheral blood; BM, bone marrow; CSF, cerebrospinal fluid. The solid bar represents CML in blast crisis exceeding 4; the hatched bar represents CML in blast crisis less than 4. (B) Hes1 expression in 5 human CML blast crisis cell lines. Expression levels of HES1 in K-562, JK-1, KCL-22, TS9:22, and JURL-MK1 were evaluated by real-time RT-PCR and were normalized by GAPDH mRNA. (C) Growth repression by transduction of dnHes1 (a dominant-negative Hes1) retrovirus vector into 3 human cell lines (K-562, TS9:22, and JURL-MK1). Six days after retrovirus transduction, cell numbers were counted. Growth is shown as a percentage of the control cells that were transduced with control vector. A representative result from 2 independent and reproducible experiments is shown. Error bars represent the SD from duplicate cultures. (D) Real-time RT-PCR for C/EBP-α in Hes1-transduced KSLs, CMPs, and GMPs compared with control vector-transduced KSLs, CMPs and GMPs. Total RNA was extracted at 60 hours from the initiation of Hes1-transduction. Error bars represent the SD from 2 independent experiments in (A-B,D).

in chronic phase patients. Although it is yet to be confirmed by a larger number of samples from CML as well as AML patients, this result indicates an interesting connection between the mouse model of AML/CML in blast crisis-like disease and human leukemia. In addition, we have demonstrated that transduction of dnHes1 represses the proliferation in 2 of 3 human cell lines of CML in blast crisis. These results suggest that Hes1 plays an important role in blast crisis of CML.

Although the origin of CML is considered to be a hematopoietic stem cell, blast crisis has been shown to be a result of transformation of myeloid progenitors.[16] BCR-ABL can cause MPN-like disease when introduced into the hematopoietic stem cell population but cannot induce MPN or leukemia when introduced into differentiated myeloid progenitors.[26] Therefore, development of full-blown AML/CML in blast crisis-like disease in mice with differentiated progenitors only by cotransduction with Hes1 and BCR-ABL may represent a true model of blast crisis of CML. In this context, Hes1 is a possible crisis-promoting gene like other examples, such as activated β-catenin[16] and BCL-2,[45] both of which caused CML in blast crisis-like disease in mice when transduced into GMPs together with BCR-ABL.

Several AML-associated fusion gene products, such as MLL-ENL,[46] MOZ-TIF2,[26] and MLL-AF9,[47] have been demonstrated to confer replating capacity on CMPs and GMPs, and eventually to transform these cells into leukemia-initiating cells. Unique to our findings is the fact that we transduced a wild-type transcription factor, Hes1, and found that such simple up-regulation of a transcription factor led to similar transformation phenotypes. A substantial number of examples have indicated that loss of function or altered function, rather than gain of function, of transcription factors, including MLL, MOZ, Runx1, RARα, C/EBP-α, etc, is associated with leukemogenesis. If up-regulation of Hes1 is indeed involved in human leukemias, this represents a new mechanism of leukemogenesis.

In modeling CML in mice, the present model provides a powerful tool by which we can induce 2 distinct phases of CML from stem cells or progenitors using BCR-ABL gene: a chronic phase-like state by transduction of KSL with BCR-ABL alone and a blast crisis-like state by cotransduction of CMPs and GMPs with BCR-ABL and Hes1.

In conclusion, we have developed a useful mouse model for CML blast crisis and have indicated that Hes1 is a key molecule in blast crisis transition in CML. The present mouse model will aid

Table 1. Clinical data of 20 patients with CML in blast crisis

Sample name	Source	Blast ratio	Hes1/GAPDH	Phenotype	Chromosome aberration	Clinical features
228 CML BC	PB	57	0.49	B-ALL	46,XY,t(9;22)/46,XY, +der(1;14)(q10;q12),t(9;22)	—
428 CML BC	PB	100	0.27	B-ALL	t(9;22)	—
984 CML BC	PB	60	0.56	B-ALL	46, XX, t(9;22)(q34;q11.2)	—
3259 CML BC	PB	100	0.16	B-ALL	t(9;22)	—
1385 CML BC	BM	81	0.56	B-ALL	t(9;22)	—
1107 CML BC	CSF	100	4.16	B-ALL	t(9;22)	The blasts increased drastically in CNS.
1 CML BC	PB	90	0.51	Myeloid	t(9;22)	—
219 CML BC	PB	12	19.72	Myeloid	45,XX,-7,t(9;22)	BM was dry tap composed of 100% blasts.
393 CML BC	PB	20	0.08	Myeloid	46,XX,t(9;22),add(17)(p11)	—
1088 CML BC	PB	30	6.22	Myeloid	46, XX, t(9;22)(q34;q11.2)	BM was dry tap.
1299 CML BC	PB	20	7.35	Myeloid	t(9;22)	BM was dry tap composed of 23% blasts.
1824 CML BC	PB	51	1.15	Myeloid	t(9;22)	BM was dry tap.
3153 CML BC	PB	7	0.66	Myeloid	t(9;22)	BM was dry tap. The blasts in BM increased up to 42% after taking this sample.
232 CML BC	BM	11	7.96	Myeloid	47,XY,+8,t(9;22)	The blasts in BM increased drastically up to 44% after taking this sample.
452 CML BC	BM	54	2.01	Myeloid	46,dic(17)(q10),t(9;22)	—
916 CML BC	BM	24	0.11	Myeloid	t(9;22)	—
1091 CML BC	BM	28	0.67	Myeloid	t(9;22)	—
811 CML BC	BM	25	26.25	Myeloid	46, XX, t(1;9;22)(q44;q34;q11.2)	—
3332 CML BC	BM	22	4.17	Myeloid	t(9;22)	—
3847 CML BC	BM	62	4.79	Myeloid	t(9;22)	—

CML indicates chronic myelogenous leukemia; BC, blast crisis; PB, peripheral blood; B-ALL, B-cell acute lymphoblastic leukemia; BM, bone marrow; CSF, cerebrospinal fluid; —, not applicable; and CNS, central nervous system.

understanding of the molecular mechanisms underlying blast crisis of CML and might lead to a better therapeutic outcome for this difficult disease.

Acknowledgments

The authors thank Dr R. Kageyama for the Hes1 cDNA; Dr H. Nakauchi and Dr M. Onodera for the GCDNsam/IRES-NGFR vector and the GCDNsam/IRES-GFP vector; Dr K. Akashi and Dr S. Mizuno for mouse C/EBP-α cDNA; Dr T. Inaba and Dr H. Asou (Hiroshima University, Hiroshima, Japan) for the JK-1, KCL-22, JURL-MK1 cell line; and Kirin Pharma for the TPO.

This work was supported by a Grant-in-Aid for Scientific Research (KAKENHI no. 20249051) and the Global Center of Excellence Program Center of Education and Research for the Advanced Genome-Based Medicine (for personalized medicine and the control of worldwide infectious diseases); the Ministry of Education, Culture, Sports, Science, and Technology of Japan (MEXT) and the Ministry of Health and Welfare of Japan (T.K.); and KAKENHI (no. 19390258), Astellas Foundation for Research on Metabolic Disorders, Uehara Memorial Foundation, and Princess Takamatsu Cancer Research Fund (S.C.).

Authorship

Contribution: F.N. did all the experiments and participated actively in writing the manuscript; M.S.-Y. and J.K. assisted with the experiments and actively participated in designing the experiments; Y.K., N.K., T.U., K.H., and K.K. assisted with the experiments; Y.H. and H.H. provided human samples; S.O. and M.K. participated in interpretation and designing the experiments; and T.K. and S.C. conceived the project, secured funding, and actively participated in manuscript writing.

Conflict-of-interest disclosure: T.K. serves as a consultant for R&D Systems and Rigel Pharmaceuticals. The remaining authors declare no competing financial interests.

Correspondence: Toshio Kitamura, Division of Stem Cell Signaling, Center for Stem Cell Therapy, Institute of Medical Science, University of Tokyo, 4-6-1 Shirokanedai, Minato-ku, Tokyo 108-8639, Japan; e-mail: kitamura@ims.u-tokyo.ac.jp; and Shigeru Chiba, Department of Hematology, Graduate School of Comprehensive Human Sciences, University of Tsukuba, 1-1-1 Tennodai, Tsukuba, Ibaraki 305-8575, Japan; e-mail: schiba-tky@umin.net.

References

1. Kageyama R, Nakanishi S. Helix-loop-helix factors in growth and differentiation of the vertebrate nervous system. *Curr Opin Genet Dev.* 1997;7(5):659-665.
2. Jarriault S, Brou C, Logeat F, Schroeter EH, Kopan R, Israel A. Signalling downstream of activated mammalian Notch. *Nature.* 1995;377(6547):355-358.
3. Jarriault S, Le Bail O, Hirsinger E, et al. Delta-1 activation of notch-1 signaling results in HES-1 transactivation. *Mol Cell Biol.* 1998;18(12):7423-7431.
4. Johnson JE, Birren SJ, Anderson DJ. Two rat homologues of Drosophila achaete-scute specifically expressed in neuronal precursors. *Nature.* 1990;346(6287):858-861.
5. Sumazaki R, Shiojiri N, Isoyama S, et al. Conversion of biliary system to pancreatic tissue in Hes1-deficient mice. *Nat Genet.* 2004;36(1):83-87.
6. Kumano K, Chiba S, Shimizu K, et al. Notch1 inhibits differentiation of hematopoietic cells by sustaining GATA-2 expression. *Blood.* 2001;98(12):3283-3289.
7. Kunisato A, Chiba S, Nakagami-Yamaguchi E, et al. HES-1 preserves purified hematopoietic stem cells ex vivo and accumulates side population cells in vivo. *Blood.* 2003;101(5):1777-1783.
8. Kaneta M, Osawa M, Sudo K, Nakauchi H, Farr AG, Takahama Y. A role for pref-1 and HES-1 in thymocyte development. *J Immunol.* 2000;164(1):256-264.
9. Tomita K, Hattori M, Nakamura E, Nakanishi S, Minato N, Kageyama R. The bHLH gene Hes1 is essential for expansion of early T cell precursors. *Genes Dev.* 1999;13(9):1203-1210.
10. Weng AP, Ferrando AA, Lee W, et al. Activating mutations of NOTCH1 in human T cell acute lymphoblastic leukemia. *Science.* 2004;306(5694):269-271.
11. Lee S-y, Kumano K, Nakazaki K, et al. Gain-of-function mutations and copy number increases of

Notch2 in diffuse large B-cell lymphoma. *Cancer Sci.* 2009;100(5):920-926.

12. Radtke F, Wilson A, Mancini SJ, MacDonald HR. Notch regulation of lymphocyte development and function. *Nat Immunol.* 2004;5(3):247-253.
13. Allman D, Punt JA, Izon DJ, Aster JC, Pear WS. An invitation to T and more: notch signaling in lymphopoiesis. *Cell.* 2002;109[suppl]:S1-S11.
14. Radtke F, Wilson A, Stark G, et al. Deficient T cell fate specification in mice with an induced inactivation of Notch1. *Immunity.* 1999;10(5):547-558.
15. Sakata-Yanagimoto M, Nakagami-Yamaguchi E, Saito T, et al. Coordinated regulation of transcription factors through Notch2 is an important mediator of mast cell fate. *Proc Natl Acad Sci U S A.* 2008;105(22):7839-7844.
16. Jamieson CH, Ailles LE, Dylla SJ, et al. Granulocyte-macrophage progenitors as candidate leukemic stem cells in blast-crisis CML. *N Engl J Med.* 2004; 351(7):657-667.
17. Akashi K, Traver D, Miyamoto T, Weissman IL. A clonogenic common myeloid progenitor that gives rise to all myeloid lineages. *Nature.* 2000; 404(6774):193-197.
18. Honda H, Fujii T, Takatoku M, et al. Expression of p210bcr/abl by metallothionein promoter induced T-cell leukemia in transgenic mice. *Blood.* 1995; 85(10):2853-2861.
19. Kitamura T, Koshino Y, Shibata F, et al. Retrovirus-mediated gene transfer and expression cloning: powerful tools in functional genomics. *Exp Hematol.* 2003;31(11):1007-1014.
20. Morita S, Kojima T, Kitamura T. Plat-E: an efficient and stable system for transient packaging of retroviruses. *Gene Ther.* 2000;7(12):1063-1066.
21. Sang L, Coller HA, Roberts JM. Control of the reversibility of cellular quiescence by the transcriptional repressor HES1. *Science.* 2008; 321(5892):1095-1100.
22. Hopfer O, Zwahlen D, Fey MF, Aebi S. The Notch pathway in ovarian carcinomas and adenomas. *Br J Cancer.* 2005;93(6):709-718.
23. Iwasaki H, Mizuno S, Mayfield R, et al. Identification of eosinophil lineage-committed progenitors in the murine bone marrow. *J Exp Med.* 2005; 201(12):1891-1897.
24. Ono R, Nakajima H, Ozaki K, et al. Dimerization of MLL fusion proteins and FLT3 activation synergize to induce multiple-lineage leukemogenesis. *J Clin Invest.* 2005;115(4):919-929.
25. Kawamata S, Du C, Li K, Lavau C. Overexpression of the Notch target genes Hes in vivo induces lymphoid and myeloid alterations. *Oncogene.* 2002;21(24):3855-3863.
26. Huntly BJ, Shigematsu H, Deguchi K, et al. MOZ-TIF2, but not BCR-ABL, confers properties of leukemic stem cells to committed murine hematopoietic progenitors. *Cancer Cell.* 2004;6(6):587-596.
27. Lozzio CB, Lozzio BB. Human chronic myelogenous leukemia cell-line with positive Philadelphia chromosome. *Blood.* 1975;45(3):321-334.
28. Okuno Y, Suzuki A, Ichiba S, et al. Establishment of an erythroid cell line (JK-1) that spontaneously differentiates to red cells. *Cancer.* 1990;66(7): 1544-1551.
29. Kubonishi I, Miyoshi I. Establishment of a Ph1 chromosome-positive cell line from chronic myelogenous leukemia in blast crisis. *Int J Cell Cloning.* 1983;1(2):105-117.
30. Gotoh A, Miyazawa K, Ohyashiki K, et al. Tyrosine phosphorylation and activation of focal adhesion kinase (p125FAK) by BCR-ABL oncoprotein. *Exp Hematol.* 1995;23(11):1153-1159.
31. Di Noto R, Luciano L, Lo Pardo C, et al. JURL-MK1 (c-kit(high)/CD30-/CD40-) and JURL-MK2 (c-kit(low)/CD30+/CD40+) cell lines: 'two-sided' model for investigating leukemic megakaryocytopoiesis. *Leukemia.* 1997;11(9):1554-1564.
32. Lee SY, Kumano K, Masuda S, et al. Mutations of the Notch1 gene in T-cell acute lymphoblastic leukemia: analysis in adults and children. *Leukemia.* 2005;19(10):1841-1843.
33. Allenspach EJ, Maillard I, Aster JC, Pear WS. Notch signaling in cancer. *Cancer Biol Ther.* 2002;1(5):466-476.
34. Fu L, Kogoshi H, Nara N, Tohda S. NOTCH1 mutations are rare in acute myeloid leukemia. *Leuk Lymphoma.* 2006;47(11):2400-2403.
35. Ingram WJ, McCue KI, Tran TH, Hallahan AR, Wainwright BJ. Sonic Hedgehog regulates Hes1 through a novel mechanism that is independent of canonical Notch pathway signalling. *Oncogene.* 2008;27(10):1489-1500.
36. Kamakura S, Oishi K, Yoshimatsu T, Nakafuku M, Masuyama N, Gotoh Y. Hes binding to STAT3 mediates crosstalk between Notch and JAK-STAT signalling. *Nat Cell Biol.* 2004;6(6):547-554.
37. Nerlov C. C/EBPalpha mutations in acute myeloid leukaemias. *Nat Rev Cancer.* 2004;4(5):394-400.
38. Gombart AF, Hofmann WK, Kawano S, et al. Mutations in the gene encoding the transcription factor CCAAT/enhancer binding protein alpha in myelodysplastic syndromes and acute myeloid leukemias. *Blood.* 2002;99(4):1332-1340.
39. Smith ML, Cavenagh JD, Lister TA, Fitzgibbon J. Mutation of CEBPA in familial acute myeloid leukemia. *N Engl J Med.* 2004;351(23):2403-2407.
40. Zhang P, Iwasaki-Arai J, Iwasaki H, et al. Enhancement of hematopoietic stem cell repopulating capacity and self-renewal in the absence of the transcription factor C/EBP alpha. *Immunity.* 2004;21(6):853-863.
41. Koschmieder S, Halmos B, Levantini E, Tenen DG. Dysregulation of the C/EBPalpha differentiation pathway in human cancer. *J Clin Oncol.* 2009;27(4):619-628.
42. Kirstetter P, Schuster MB, Bereshchenko O, et al. Modeling of C/EBPalpha mutant acute myeloid leukemia reveals a common expression signature of committed myeloid leukemia-initiating cells. *Cancer Cell.* 2008;13(4):299-310.
43. Fan X, Mikolaenko I, Elhassan I, et al. Notch1 and notch2 have opposite effects on embryonal brain tumor growth. *Cancer Res.* 2004;64(21): 7787-7793.
44. Hallahan AR, Pritchard JI, Hansen S, et al. The SmoA1 mouse model reveals that notch signaling is critical for the growth and survival of sonic hedgehog-induced medulloblastomas. *Cancer Res.* 2004;64(21):7794-7800.
45. Jaiswal S, Traver D, Miyamoto T, Akashi K, Lagasse E, Weissman IL. Expression of BCR/ABL and BCL-2 in myeloid progenitors leads to myeloid leukemias. *Proc Natl Acad Sci U S A.* 2003;100(17):10002-10007.
46. Cozzio A, Passegue E, Ayton PM, Karsunky H, Cleary ML, Weissman IL. Similar MLL-associated leukemias arising from self-renewing stem cells and short-lived myeloid progenitors. *Genes Dev.* 2003;17(24):3029-3035.
47. Krivtsov AV, Twomey D, Feng Z, et al. Transformation from committed progenitor to leukaemia stem cell initiated by MLL-AF9. *Nature.* 2006;442(7104): 818-822.

Leukemia (2010) 24, 1018–1024

www.nature.com/leu

ORIGINAL ARTICLE

AID-induced T-lymphoma or B-leukemia/lymphoma in a mouse BMT model

Y Komeno[1,2], J Kitaura[1,2], N Watanabe-Okochi[3,4], N Kato[1,2], T Oki[1,2], F Nakahara[1,2], Y Harada[5], H Harada[6], R Shinkura[7], H Nagaoka[7], Y Hayashi[8], T Honjo[7] and T Kitamura[1,2]

[1]Division of Cellular Therapy, Advanced Clinical Research Center, Institute of Medical Science, University of Tokyo, Minato-ku, Tokyo, Japan; [2]Division of Stem Cell Signaling, Center for Stem Cell Therapy, Institute of Medical Science, University of Tokyo, Minato-ku, Tokyo, Japan; [3]Department of Hematology and Oncology, Graduate School of Medicine, University of Tokyo, Bunkyo-ku, Tokyo, Japan; [4]Department of Transfusion Medicine, Graduate School of Medicine, University of Tokyo, Bunkyo-ku, Tokyo, Japan; [5]International Radiation Information Center, Research Institute for Radiation Biology and Medicine, Hiroshima University, Minami-ku, Hiroshima, Japan; [6]Department of Hematology and Oncology, Research Institute for Radiation Biology and Medicine, Hiroshima University, Minami-ku, Hiroshima, Japan; [7]Department of Immunology and Genomic Medicine, Graduate School of Medicine, Kyoto University, Sakyo-ku, Kyoto, Japan and [8]Department of Hematology/Oncology, Gunma Children's Medical Center, Shibukawa, Gunma, Japan

Activation-induced cytidine deaminase (AID) diversifies immunoglobulin through somatic hypermutation (SHM) and class-switch recombination (CSR). AID-transgenic mice develop T-lymphoma, indicating that constitutive expression of AID leads to tumorigenesis. Here, we transplanted mouse bone marrow cells transduced with AID. Twenty-four of the 32 recipient mice developed T-lymphoma 2–4 months after the transplantation. Surprisingly, unlike AID-transgenic mice, seven recipients developed B-leukemia/lymphoma with longer latencies. None of the mice suffered from myeloid leukemia. When we used nude mice as recipients, they developed only B-leukemia/lymphoma, presumably due to lack of thymus. Analysis of AID mutants suggested that an intact form with SHM activity is required for maximum ability of AID to induce lymphoma. Except for a K-ras active mutant in one case, specific mutations could not be identified in T-lymphoma; however, Notch1 was constitutively activated in most cases. Importantly, truncations of Ebf1 or Pax5 were observed in B-leukemia/lymphoma. In conclusion, this is the first report on the potential of AID overexpression to promote B-cell lymphomagenesis in a mouse model. Aberrant expression of AID in bone marrow cells induced leukemia/lymphoma in a cell-lineage–dependent manner, mainly through its function as a mutator.
Leukemia (2010) **24,** 1018–1024; doi:10.1038/leu.2010.40;
published online 1 April 2010
Keywords: AID; BMT; T-lymphoma; B-leukemia/lymphoma

Introduction

Under physiological conditions, activation-induced cytidine deaminase (AID) is expressed in germinal center (GC) B-cells and initiates somatic hypermutation (SHM) and class-switch recombination (CSR) by deaminating a cytosine to create a uracil.[1,2] Structurally, the N-terminal or C-terminal domain of AID is indispensable for SHM or CSR, respectively.[3–5] Interestingly, expression of AID is increased in B-lymphoid leukemia or GC-derived B-lymphoma, with frequent hypermutation of proto-oncogenes and reciprocal chromosomal translocation.[6–9] In fact, recent studies have shown that AID is required for GC-derived lymphomagenesis and c-Myc/IgH chromosomal translocations.[10,11] In addition, elevated expression of endogenous AID and aberrant somatic mutations in tumor-related genes have also been observed in cancerous tissues related to inflammation.[12] Analysis of AID-transgenic (Tg) mice has revealed that constitutive expression of AID leads to tumorigenesis; ubiquitous and constitutive expression of AID induced lethal T-lymphoma with no apparent chromosomal translocation, occasionally accompanied by lung, liver, and gastric cancers,[13,14] and specific expression of AID in double-positive thymocytes also induced T-lymphoma.[15] However, neither AID-Tg mice specifically expressing AID in single-positive thymocytes and mature T-cells nor AID-Tg mice with CD19$^+$ B-cell-specific expression of AID developed lymphoma/leukemia.[15,16] These results suggest that susceptibility to AID-induced tumorigenesis depends on tissue or cell lineage, but the underlying mechanism remains obscure. Importantly, sequencing analysis in AID-Tg mice indicated that AID is an organ-specific mutator of non-Ig genes.[14] To prevent accumulation of unfavorable mutations induced by AID, its activity is tightly regulated by several mechanisms.[17]

In this study, we focused on AID-mediated leukemogenesis and created a mouse bone marrow transplantation (BMT) model, using BM cells retrovirally transduced with AID. Notably, recipient mice developed B-leukemia/lymphoma, albeit less frequently as compared with thymic T-lymphoma.

Correspondence: Dr T Kitamura, Division of Cellular Therapy, Advanced Clinical Research Center, Institute of Medical Science, University of Tokyo, 4-6-1 Shirokanedai, Minato-ku, Tokyo 108-8639, Japan.
E-mail: kitamura@ims.u-tokyo.ac.jp
Received 23 November 2009; revised 8 January 2010; accepted 9 February 2010; published online 1 April 2010

Materials and methods

Retroviral constructs, transfection, and retrovirus production

Murine AID (mAID), mAID mutants (G23S[4] and Δ189–198[5]), human AID (hAID), and hAID mutants (P20[3] and JP8B[3]) were subcloned into the pMYsIG vector as described in 'Supplementary Materials and methods'. All constructs were verified by DNA sequencing. Expression of wild-type or mutant AID was recognized in 293T cells transiently transfected with each construct. Retroviruses were generated by transient transfection of Plat-E packaging cells with FuGene 6 (Roche Diagnostics, Mannheim, Germany), as described earlier.[18–20]

Mouse BMT

Mouse BMT was performed as described earlier.[20] C57BL/6 CD45.1 or CD45.2 mice were used as donors or recipients,

respectively. Infected cells (2×10^5) were intravenously injected into recipient mice, which had been administered a sublethal dose of γ-irradiation. Overall survival was estimated using the Kaplan–Meier method and log-rank test. Data are presented as the means ± s.d. PB smears and cytospin slides were stained with Hemacolor (Merck, Darmstadt, Germany). Tissues were fixed in 4% w/v buffered formalin, embedded in paraffin, and then sliced and stained with standard hematoxylin and eosin. All animal studies were approved by the Animal Care Committee of the Institute of Medical Science, The University of Tokyo.

Flow cytometric analysis

Cells were stained with phycoerythrin-conjugated monoclonal antibodies (eBiosciences, San Diego, CA, USA), as described.[20] Flow cytometric analysis was performed with a FACSCalibur equipped with CellQuest software (BD Biosciences, San Jose, CA, USA) and Flowjo software (Tree Star, San Carlos, CA, USA).

Western blotting

Equal numbers of cells were denatured in pre-heated sample buffer. Western blotting was performed as described.[20] Anti-AID mAb raised against the N-terminus of mAID, and anti-α-tubulin Ab (T6074, Sigma-Aldrich, St Louis, MO, USA) were used.

Southern blotting

Southern blotting was performed as described.[20] Briefly, 10 μg of genomic DNA digested with *EcoRI* was electrophoresed on a 0.7% agarose gel. Proviruses were probed with a ^{32}P-labeled GFP probe.

Reverse transcription and real-time PCR

Real-time PCR was performed using LightCycler (Roche Diagnostics), as described.[20] cDNA was amplified using a SYBR Premix EX Taq (Takara, Shiga, Japan). Primer pairs and conditions used for real-time PCR are listed in 'Supplementary Materials and methods'. Informed consent for the use of the human leukemia/lymphoma cells was obtained from patients in accordance with the Declaration of Helsinki, and study approval was obtained from the ethics committee of the Institute of Medical Science, the University of Tokyo (Approval Number 20-10-0620).

Sequencing of target genes

Genomic PCR was performed by using AmpliTaq Gold (Roche Molecular Systems Inc., Branchburg, NJ, USA) and the primer pairs described in 'Supplementary Materials and methods'. The PCR products were gel-purified and directly sequenced. If necessary, PCR products were subcloned and sequenced.

Treatment of AID-induced T-lymphoma cell lines with γ-secretase inhibitor

Cell lines of AID-induced T-lymphoma were established by culturing tumor cells in RPMI1640 with 20% FBS. Human T-acute lymphoblastic leukemia (T-ALL) cell lines Jurkat and HPB-ALL were cultured in RPMI1640 with 10% FBS. Various concentrations of γ-secretase inhibitor (DAPT, 565770, Calbiochem, Darmstadt, Germany) or vehicle (DMSO, Wako, Osaka, Japan) were added to 5×10^3 cells for 72 h. Cell growth was estimated by using CellTiter-Glo (Promega, Madison, WI, USA). Cleavage of intracellular domains of Notch1 (ICN) was detected by anti-ICN antibody (2421, Cell Signaling, Beverly, MA, USA) in western blotting.

Results

Transduction with AID into BM cells causes B-leukemia/lymphoma as well as thymic T-lymphoma in a mouse BMT model

First, we asked whether transduction of wild-type mAID (WT) into BM cells caused leukemia/lymphoma other than T-lymphoma in a BMT model ($n = 32$) (Figure 1). We confirmed efficient retrovirus infection: 50–70% and 76–84% of the BM cells transduced with WT or mock, respectively, were GFP-positive before transplantation. The recipient mice of WT-transduced cells developed thymic T-lymphoma more frequently than did AID-Tg mice[13] (75 vs 35%). The disease was associated with hepatosplenomegaly, killing the mice in 2–4 months after transplantation (Figure 1a; Supplementary Figure 1; Supplementary Table 1). Histological and flow cytometric analyses showed that the thymus was filled with the T-lymphoblastic cells CD3^{dull}, CD4$^+$, CD8$^+$, and Thy1.2$^+$, indicating the differentiation block at early stages of T-cell development in thymus (Figures 1b–d). The complete blood counts of these mice were usually normal, except for the increase of T-lymphoblastic cells or mature granulocytes in some cases (Supplementary Figure 1; Supplementary Table 1, and data not shown). Notably, 7 of 32 transplanted mice (22%) developed B-leukemia/lymphoma with pancytopenia and splenomegaly, and died with significantly longer latencies as compared with those of T-lymphoma (Figures 1a–d; Supplementary Figure 1; Supplementary Table 1). Spleen and BM were filled with B-lymphoblastic cells in most cases, while affected lymph nodes differed in size among cases. B-lymphoma cells were B220$^+$, CD19$^+$, CD43$^{dull/+}$, c-kit$^{dull/+}$, and IgM$^-$ (Figure 1d). Neither Bcl-6 induction[21,22] nor abnormal Ikaros deletions[23] were detected in these cells (data not shown). There was a wide range of GFP-positive ratios among AID-induced T- or B-lymphoma cells, irrespective of disease severity (Supplementary Figure 2 and data not shown). Sequencing analysis of GFP gene integrated into the genome revealed multiple mutations, resulting in reduced green fluorescence. Interestingly, one recipient developed both T- and B-lymphoma. None of the mice suffered from myeloid leukemia. The lymphoma cells, irrespective of T- or B-lineage, were serially transplantable and developed T- or B-leukemia with shorter latencies, respectively (data not shown). The recipient mice of mock-transduced cells did not develop any leukemia/lymphoma (Figure 1a). Collectively, transduction with AID into BM cells led to thymic T-lymphoma or B-leukemia/lymphoma, but not myeloid leukemia in a mouse BMT model. Similar results were obtained when Balb/c mice were used (data not shown).

We next asked whether the integration of retroviruses influenced the different phenotypes (T- or B-lymphoma) in AID-induced leukemogenesis. Southern blot analysis demonstrated a single or several proviral integrations in T-lymphoma samples (Figure 1e, left panel). On the other hand, we found that a single integration was predominant in B-lymphoma samples (Figure 1e, right panel). In one recipient harboring both T- and B-lymphoma, a distinct integration was confirmed in each sample (Figure 1e, right panel, lanes *B and *T), indicating the double cancer in this case. We identified a single or several retroviral integration sites (RIS) from lymphoma samples by inverse PCR method (Supplementary Table 2). However, we could not find any specific relationship between RIS and different phenotypes of lymphomas. In addition, a common integration site was identified only in one recipient (ID69) (Supplementary Table 2). These results suggested that AID-induced lymphomagenesis mainly depended on its intrinsic function, but not RIS.

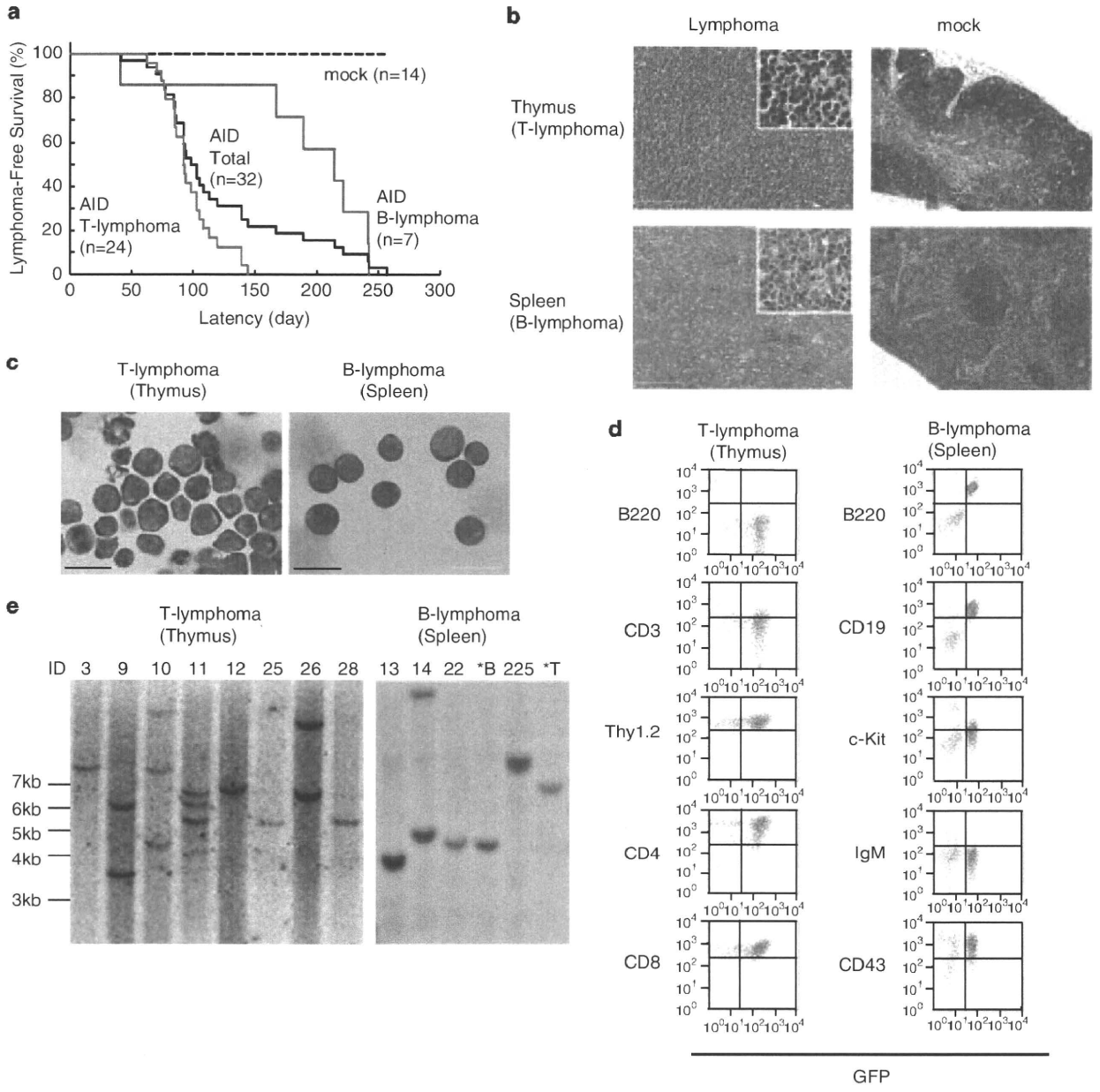

Figure 1 AID-induced T-lymphoma and B-leukemia/lymphoma in a mouse BMT model. (**a**) Kaplan–Meier plot of survival (black lines). Survival curve for AID recipient mice that developed T-lymphoma or B-lymphoma is indicated by green or red line, respectively. (**b**) Hematoxylin and eosin staining of AID-induced T-lymphoma (thymus, upper/left panel), control thymus (upper/right panel), AID-induced B-lymphoma (spleen, lower/left panel), or control spleen (lower/right panel). Magnifications ×200 (overview) and ×400 (insert). Scale bars: 200 μm. (**c**) Cytospin preparations of T-lymphoma (left panel) and B-lymphoma (right panel). Magnification ×1000. Scale bars: 20 μm. (**d**) Flow cytometric analysis of lymphoma cells. (**e**) Southern blotting of T-lymphoma (left panel) and B-lymphoma (right panel). *B or *T in the right panel indicates B- or T-lymphoma, respectively, which was found in the same mouse (ID 29).

We then asked whether other hematopietic malignancies, including myeloid leukemia, are induced in the absence of thymus. We used athymic nude mice as recipients of a BMT model, finding that 5 of 8 nude mice transplanted with AID-transduced BM cells developed B-leukemia/lymphoma, but no other hematopoietic diseases were observed (Supplementary Figure 3). Thus, B-leukemia/lymphoma was predominantly induced in the absence of thymus, but transduction of AID into BM cells did not induce myeloid leukemia. Altogether, these results suggested that the oncogenic transformation of AID-transduced BM cells requires *in vivo* environment suitable for differentiation and proliferation of immature lymphoid cells.

Impaired lymphomagenesis by SHM-defective AID mutants

To examine how SHM and/or CSR activities of AID contribute to lymphomagenesis, we constructed a BMT model using mutant forms of AID: missense mutant G23S with decreased SHM activity[4]; and truncation mutant Δ189–198 defective for CSR